

A novel anaerobic membrane bioreactor with magnetotactic bacteria for organic sulfur pesticide wastewater treatment: Improvement of enzyme activities, refractory pollutants removal and methane yield

Shiming Cui ^{a,b}, Dongxue Hu ^{a,b,*}, Zhaobo Chen ^{a,b}, Yifan Wang ^{a,b}, Jitao Yan ^{a,b}, Shuya Zhuang ^{a,b}, Bei Jiang ^{a,b}, Hui Ge ^{a,b}, Zihan Wang ^{a,b}, Pengcheng Zhang ^{a,b}

^a Key Laboratory of Biotechnology and Bioresources Utilization, Ministry of Education, Dalian Minzu University, 18 Liaohe Road West, Dalian Economic and Technological Development Zone, Dalian 116600, China

^b College of Environment and Resources, Dalian Minzu University, 18 Liaohe West Road, Dalian 116600, China

ARTICLE INFO

Keywords:

Anaerobic membrane bioreactor (AnMBR)
Magnetotactic bacteria (MTB)
Organic sulfur pesticide wastewater
Refractory pollutants
Enzyme activities
Methane yield

ABSTRACT

The high refractory pollutant and heavy metal content in organic sulfur pesticide wastewater limits the removal of chemical oxygen demand (COD) and methane yield of conventional anaerobic membrane bioreactors (c-AnMBRs) due to low enzyme activity. The objective of this study was to investigate the impact of magnetotactic bacteria (MTB) with excellent adsorption capabilities on the performance of the AnMBR system at different hydraulic retention times (HRTs). The MTB-assisted AnMBR (R_2) showed improved COD removal efficiency (75 %–78 %) over c-AnMBR (R_1) by 3 %–7% at HRT of 60, 48, and 36 h. Mancozeb and ethylenethiourea removal efficiencies of R_2 were 7.1 %–25.0 % and 25.2 %–28.5 % higher than R_1 , respectively. The Mn^{2+} and Zn^{2+} of R_2 were significantly reduced by $16.8 \pm 1.9\%$ and $10.0 \pm 0.8\%$ than that of R_1 , which were obtained at HRT of 36 h. The activity ratio of protease and dehydrogenase between R_1 and R_2 was 205.5 % and 419.6 %, respectively. Specific methane yield and specific methane activity of R_2 were 1.16 and 1.13 times those of R_1 , respectively. A mathematical model correlating refractory pollutants, enzyme activity, and COD removal efficiency was established. This study innovatively developed a green MTB-assisted AnMBR technology that successfully removed refractory pollutants and heavy metals while enhancing enzyme activity and methane yield, reducing toxicity threat and improving energy recovery efficiency, along with providing both scientific basis and technical foundation for low-carbon operation of pesticide wastewater treatment.

1. Introduction

Pesticides are widely applied to eliminate or control diseases, insects, weeds and other hazardous organisms, which harm agriculture and forestry. According to the data of the Ministry of Agriculture and Rural Affairs of the People's Republic of China, the national production of chemical pesticide prodrugs (100 % active ingredient) was 3.723 Mt in 2023, with an increase of 49.1 % from 2022 [1]. Pesticides can be divided into organic sulfur pesticides, organophosphorus pesticides, pyrethroids pesticides, sulfonylurea pesticides and biological pesticides, etc. Among them, organic sulfur pesticides mainly include ethylenebis-dithiocarbamate fungicides, nereistoxin insecticides, thiram fungicides, and so on. Pesticide wastewater is generated during the production of

organic sulfur pesticides. This wastewater contains refractory parent compounds such as mancozeb and ethylenethiourea (ETU), which are difficult to be degraded. In addition, the pesticide wastewater also contains various primary pollutants including Mn^{2+} , Zn^{2+} , total cyanide, nitrobenzene, and so on. The hazardous consequences of mancozeb include impaired thyroid function, neurotoxicity, and reproductive toxicity, with ETU serving as the endpoint [2]. According to the findings of in vitro research, mancozeb ought to be classified as a reproductive toxicant since it may indirectly interfere with or hinder cellular reproduction [3]. ETU is a typical biotoxic pollutant in organic sulfur pesticide wastewater, which can produce possible carcinogens in an acidic environment [4]. Previous research established that Mn^{2+} has neurotoxicity to organisms [2]. The growth of the acetoclastic and

* Corresponding author at: Key Laboratory of Biotechnology and Bioresources Utilization, Ministry of Education, Dalian Minzu University, 18 Liaohe Road West, Dalian Economic and Technological Development Zone, Dalian 116600, China.

E-mail address: hudongxue@dlnu.edu.cn (D. Hu).

hydrogenotrophic methanogens would be adversely affected by Zn^{2+} [5]. These highly toxic pollutants are discharged with the wastewater and cause extremely harsh consequences to the environment. Thus, an available technique of pollution prevention and control is urgently needed to treat organic sulfur pesticide wastewater.

Extensive research has shown that electro-Fenton oxidation, electrolytic chlorination and photocatalytic oxidation achieved good results in treating pesticide wastewater. He et al. [6] used graphite as the cathode and $Ti/RuO_2-IrO_2-SnO_2$ as the anode to catalyse the treatment of pesticide wastewater containing a high concentration of chlorine salts with 3 g/L pyrite for 3 h. The removal efficiencies of chemical oxygen demand (COD), chroma, ammonia nitrogen and total nitrogen reached 99 %, 99.8 %, 98.9 % and 46.0 %, respectively. Wang et al. [7] achieved 86.43 % COD removal efficiency and 98.67 % atrazine removal efficiency with permeate COD less than 50 mg/L and NH_4^+ -N less than 1.5 mg/L, respectively, by treating pesticide wastewater through the electrochlorination process. The percentage reduction of dieldrin and delta-methrin in agricultural wastewater following 12 h of UV irradiation at 254 nm and 306 nm wavelengths was 58.8 % and 46.8 %, and 52.9 % and 37.3 %, respectively [8]. However, these methods are costly and could cause secondary pollution which increased the difficulty of subsequent treatment [9]. Moreover, these processes treat wastewater with low concentrations of refractory pollutants or simple wastewater compositions, making them difficult to apply in practical production scenarios.

Recent pieces of evidence suggested that concentrated wastewater treatment facilities for the pesticide industry started using biochemical techniques to treat pesticide wastewater [10]. Anaerobic biological treatment techniques such as hydrolytic acidification, up-flow anaerobic sludge bed (UASB), anaerobic expanded granular sludge bed (EGSB), anaerobic internal recirculation reactor (IC) and anaerobic membrane bioreactor (AnMBR) have potential due to their characteristics of high volumetric loads and high shock-loading resistance for the treatment of pesticide wastewater. The biochemistry of mixed pesticide wastewater containing xylene and abamectin was increased from 0.08 to 0.32 after bipolar acid-base ozone pretreatment and the COD removal efficiency was about 20 % when the influent concentration reached 2150 mg/L in the subsequent anaerobic treatment [11]. Akinapally et al. [12] treated pesticide wastewater with an initial COD of 90000 mg/L using a rotary evaporation-distillation-Fenton-anaerobic digestion process, removing 55 % by anaerobic digestion, for a total removal efficiency of 95 %. Min et al. [13] set up a two-stage anaerobic process with a conventional UASB for treating pesticide wastewater with $67.2 \pm 7.9\%$ average COD removal efficiencies. In addition, AnMBR improves the removal effect while prolonging solid retention time (SRT) and decreasing hydraulic retention time (HRT) [14]. Liu et al. [15] treated diluted pesticide wastewater using AnMBR with maximum COD removal efficiencies of 80.1 %, 80.0 %, 67.4 % and 61.1 % at HRT of 96, 72, 48 and 24 h, respectively. However, far too little attention has been paid to toxic substances with high concentrations such as mancozeb, ETU and Mn^{2+} in organic sulfur pesticide wastewater, which would inhibit the microorganism activities in the AnMBR, leading to the necessity of diluting the raw pesticide wastewater before it is treated by the conventional AnMBR. Thus, an efficient strategy to reduce the toxicity of pollutants to retrofit AnMBRs for the treatment of organic sulfur pesticide wastewater is critically needed.

Magnetotactic bacteria (MTB) are a group of microaerobic or anaerobic Gram-negative microorganisms that are widespread in the oxic-anoxic transition zone of freshwater and marine habitats. Studies have established that the unique property of magnetotaxis of MTB originate from the magnetosome within the microstructure, allowing MTB to sense the north and south pole magnetic fields of the Earth and to be driven by the flagellum [16]. Using this property, MTB can be forced by magnets to move towards the magnetic field, to isolate and enrich from water bodies. One isolation technique called orientation magnetic separation can be used for the separation of motile MTB that

contain magnetic moments. This technique utilized a magnetic field to separate bacteria such as *Magnetospirillum gryphiswaldense* strain MSR-1 and *Magnetospirillum magneticum* strain AMB-1 from water using an external magnetic field [17]. The separated MTB could then be cultured on a large scale in flasks and fermenters under microaerobic conditions, which provided a basis for the application of MTB in various fields. The applications of MTB have been mainly concentrated in biomedicine, mechanics of materials, crystallography, and astrobiology, with little research in environmental engineering [18,19]. Recently investigators have shown that MTB have significant treatment effects on heavy metals and organic pollutants [17]. MTB could incorporate Mn and Zn into magnetosomes and other cellular compartments, and integrate these metals into the magnetite core of the magnetosomes [20]. In groundwater samples enriched with MTB-enriched solutions, the average removal efficiency of Mn^{2+} reached 15.26 % [21]. In another study, a consortium of magnetotactic bacteria was utilized to achieve metal recovery rates of 75 % for Zn in diodes and 47 % in resistors, respectively [22]. An additional area of interest is the potential of MTB to effectively remove the prodrugs active ingredient of pesticide. Data from prior studies indicate that genetically modified MTB may serve as a nanobiocatalyst capable of degrading 90–100 % of a 1 mL sample contaminated with 50 $\mu\text{mol}/\text{L}$ of ethyl-paraoxon, an organophosphorus pesticide, within a 2-day period [23]. In another study, AMB-1 has been utilized to remove chlorpyrifos from deionized water, river water, tap water, and culture medium, achieving removal efficiencies of 87.5 %, 86.6 %, 73.9 % and 74.7 % within 180 min in dynamic mode [24]. However, the composition of organic sulfur pesticide wastewater is more complex, whether MTB driven by the magnetic field can also maintain a superior removal efficiency of metal ions and prodrug active ingredients remains to be studied. Moreover, previous researches have not investigated combining MTB with anaerobic biological techniques to treat raw pesticide wastewater to investigate its comprehensive treatment efficacy.

According to the above studies, MTB is anticipated to remove heavy metals (Mn and Zn) and refractory pollutants (mancozeb and ETU) from pesticide wastewater. These contaminants could potentially suppress bacterial activity and reduce enzyme activity [25,26]. Therefore, integrating MTB with AnMBR could boost the elimination of such pollutants, enhancing enzyme activity and consequently improving COD removal efficiency and methane production. Moreover, decreasing the concentrations of heavy metals and refractory pollutants mitigates their stimulatory effect on microbial secretion, reducing the release of extracellular polymeric substances and soluble microbial products, which in turn mitigates membrane fouling [27].

Therefore, to address the aforementioned research gaps, in this study, a novel MTB-assisted AnMBR was established, which was combined with the MTB and magnetic field. By comparing the MTB-assisted AnMBR with the conventional AnMBR (c-AnMBR), the following aspects were systematically expressed: (1) evaluating the performance of MTB-assisted AnMBR versus c-AnMBR focusing on removing pollutants in organic sulfur pesticide wastewater, including COD, mancozeb, ETU, Mn^{2+} and Zn^{2+} under different HRTs; (2) investigating the methanogenic generation (biogas production, methane content, specific methane activity (SMA) and specific methane yield (SMY)); (3) determining the activities of protease, α -glucosidase, dehydrogenase (DHA), acetate kinase (ACK) and coenzyme F₄₂₀ in MTB-assisted AnMBR and c-AnMBR; (4) analyzing the relationship between refractory pollutants, enzyme activity and COD removal efficiency of MTB-assisted AnMBR and c-AnMBR, and offering a reference and basic data of MTB application for organic sulfur pesticide wastewater treatment.

2. Materials and methods

2.1. Organic sulfur pesticide wastewater characteristics

The influent wastewater was from an organic sulfur pesticide

industrial plant in Dalian, China, which had an acrid scent and a yellow visual. In addition to the active ingredients in pesticides such as mancozeb and ETU, Mn^{2+} , Zn^{2+} , cyanide, absorbable organic halogens (AOX), nitrobenzene, etc. were also present. The main characteristic parameters of wastewater are shown in Table 1. The influent and permeate were collected from R_1 and R_2 seven times per month for analysis. COD, BOD₅, MLSS and MLVSS were measured according to the Standard Methods for the Analysis of Water and Wastewater developed by the American Public Health Association (APHA, 2005).

Mancozeb and ETU were analyzed using a high-performance liquid chromatography (HPLC) system, including an LC-20 AB liquid chromatograph, SPD-20A UV detector, CTO-20A column heater, DGU-20A3 degasser and LC Solution workstation (Shimadzu, Japan). The specific experimental steps refer to the method of Lopez et al. [28]. For HPLC analysis, a 20 mL extract sample was introduced into a column maintained at a constant temperature of 35 °C. The chromatographic column utilized was a Thermo Hypersil ODS2 (250 mm × 50 mm, 5 µm), with a mobile phase consisting of water: acetonitrile (97:3 v/v) at a flow rate of 0.5 mL/min. Quantification of mancozeb and ETU was achieved using a diode array detector at wavelengths of 271 nm and 232 nm, respectively. Biogas was collected from the top end of the AnMBR via a hydraulic seal unit and the production was measured by syringes. The methodology for measurement was adapted from Zhao et al. [29]. Methane production was quantified using a gas chromatograph equipped with a thermal conductivity detector (TCD-GC; GC-2014, Shimadzu, Japan), which included TDX and Porapak Q chromatographic columns (AETO, China). These columns, made of stainless steel with an inner diameter of 4 mm, were 2 m in length and packed with 60/80 mesh material. During GC analysis, the temperatures of the injector, column and detector were maintained at 40 °C, 40 °C and 80 °C, respectively. Nitrogen served as the carrier gas at a flow rate of 30 mL/min. Capillary suction time (CST) of biomass was measured by CST Equipment (Model 304 M, Triton Electronics Co., Ltd., UK).

2.2. AnMBRs setup and operation

The laboratory-scale MTB-assisted AnMBR (R_2) is schematically illustrated with the c-AnMBR (R_1) in Fig. 1. Each reactor consisted of an up-flow anaerobic sludge bed (UASB) of 0.3 m height and 0.05 m inside diameter and a membrane tank with a total working volume of 2.2 L. The influent entered the bottom of the UASB through a PLC-controlled (programmable logic controller) feed pump with constant flow via a flowmeter. Moreover, a three-phase separator at the top of the UASB separated the biogas, wastewater and sludge. Simultaneously, most of the sludge settled back to the bottom of the UASB while a small portion flowed into the membrane tank and was returned by the recirculation pump. The treated wastewater was further filtered through the membrane module and finally pumped into the permeate tank. The membrane module in the membrane tank was a hollow fibre curtain membrane (LS-005, Shanghai Lishui Environmental Protection Equipment Co. Ltd., China), which was made of polyvinylidene fluoride (PVDF) with a 35 mm thickness of membrane fibres, a surface area of 45 cm², 2.05 mm outer diameter and 0.1–0.2 µm membrane aperture. In addition, the membrane module was operated by negative pressure suction, and the permeate cycle was: 8 min out and 2 min off. Experimental trials were conducted by operating four stages at HRTs of 60, 48, 36 and 24 h, corresponding to filtration fluxes of 8, 10, 13.1 and 20 L/m²·h, respectively. The transmembrane pressure (TMP) was monitored by a vacuum pressure gauge. Water in the permeate tank was used for backwashing. The membranes were backwashed at a frequency of once every 30 min, with each backwash lasting 5 s to control the membrane fouling. Chemical cleaning agents (HCl, Citric acid, NaOH and NaClO) were used to chemically clean the membrane components when TMP was over 50 kPa.

The external magnetic field setup for R_2 was as follows: three turntables were equipped with NdFeB magnets with dimensions of 40 × 40

× 10 mm, and two magnets with a central magnetic field strength of about 500 mT were placed symmetrically on each turntable (Fig. 1b). When the turntable stopped, the total six magnets were aligned on the same horizontal line with the poles facing the same direction. Afterwards, PLC controlled the turntables to rotate 180° every hour and converted the position of the magnet to reverse the magnetic field, which caused the MTB to move directionally to the opposite side. When the turntables were stopped, the magnets stayed at the closest points to the exterior surface of the UASB and the membrane tank.

R_1 and R_2 were operated for 330 days (d). The operating temperature was keeping 25 ± 1 °C (except for causing by electrical problems), and pH was varied from 6 to 8. Besides, the other specific conditions of operation for each stage are displayed in Table 2. Especially, due to the excessive production of pesticide factories, the concentrations of various pollutants have reached their peaks from 122 to 130 d, with 18000 mg/L COD, 5200 mg/L mancozeb, 2000 mg/L ETU and 5000 mg/L Mn^{2+} . The impact of high-concentration pollutants caused different negative effects on the two reactors; therefore, from 143 to 164 d, the influent COD concentration was diluted to gradually restore the performance of the reactors.

2.3. Sludge characterisation and MTB cultivation

R_1 and R_2 were inoculated with mixed sludge from the following sources: anaerobic digesters of a municipal domestic wastewater treatment plant (MLSS = 12.5 g/L, MLVSS = 8.5 g/L, MLVSS/MLSS = 0.68), a brewery wastewater treatment plant (MLSS = 35.8 g/L, MLVSS = 25.8 g/L, MLVSS/MLSS = 0.72) and a chemical plant wastewater treatment plant (MLSS = 18.6 g/L, MLVSS = 11.5 g/L, MLVSS/MLSS = 0.62) mixed on a 1:2:2 vol ratio. Moreover, the mixed sludge had an initial MLSS of 18.3 g/L and an initial MLVSS of 11.7 g/L, with MLVSS/MLSS = 0.64. Sludge samples were collected from ports located at the heights of 0.03, 0.08 and 0.15 m above the bottom, corresponding to the sludge bed zone, suspended sludge zone and settling zone, respectively. Furthermore, the adsorption test utilized sludge samples, as provided in Text S2 of the Supplementary materials.

Water samples and sea mud were collected from Mazumiao Beach in Dalian, and the MTB were isolated and cultured by using different media. The water-mud mixtures were put into 500 mL food-grade plastic bottles with screw caps at a ratio of 1:2, then placed in a constant temperature incubator at 25 °C and protected from light for static cultivation. After four or five weeks, the bottles were magnetised by the magnets for 30 min. Subsequently, the magnetically sensitive organisms were collected by Pasteur pipettes. Following that, the organisms were added to the Petri dishes containing the isolation medium (Table S1) in the laminar flow cabinet. Incubated the Petri dishes with magnetic fields in an incubator at 25 °C for 2–3 days until single colonies appeared, then picked and isolated them until pure MTB colonies were obtained. Then MTB were picked out from the isolation medium with an inoculating ring, transferred to the growth medium (Table S2) and incubated in a freezing shaker at 25 °C. After 24 h, the white substance at the bottom of the bottles was the cultured MTB. 1.1 g/L cultured MTB and mixed sludge were inoculated together to the reactors for acclimation. The acclimation was carried out for 50 d, with HRT of 120 h. The COD influent concentration increased gradually, from 3000 to 11000 mg/L in the first 20 d, then was kept at about 11000 mg/L in the last 30 d. Finally, the COD removal efficiency was higher than 70 %, which indicated that the reactor had been started successfully.

2.4. Enzyme activities and SMA test

Four days (52, 96, 275 and 306 d) of water samples in reactors were selected to determine the enzyme activity to represent the average level of each stage after stable operation. Three sets of parallel experiments were conducted for all assays and the results were averaged thereafter. The assays for protease and α -glucosidase activities were based on Goel

Table 1

Characteristics of organic sulfur pesticide wastewater.

Parameter	Value	Parameter	Value
COD (mg/L)	3273–18623	Mancozeb (mg/L)	1516–5240
BOD ₅ (mg/L)	720–2980	Ethylenethiourea (mg/L)	805–2050
BOD ₅ /COD	0.16–0.24	Mn ²⁺ (mg/L)	2631–5018
TN (mg/L)	260–540	Zn ²⁺ (mg/L)	0.23–0.29
NH ₄ ⁺ -N (mg/L)	120–250	Nitrobenzeno(mg/L)	17–35
TP (mg/L)	3–12	Chlorides (mg/L)	58–124
VFA (mg/L)	96–541	Sulphates (mg/L)	900–5300
Alkalinity (mg/L)	1200–2800	Total cyanide(mg/L)	290–770
Suspended solids (mg/L)	500–3800	pH	6–8

et al. [30]. Briefly, protease activity was determined by centrifugation of azo casein after degradation to tyrosine at pH = 8 for 30 min, mixing with 2 M NaOH, and finally measuring the absorbance of the resulting coloured compound at 440 nm. The quantity of enzyme that caused a rise in absorbance of 0.01 at 440 nm was designated as one unit of protease activity (IU). While α-glucosidase degraded *p*-nitrophenyl-α-D-glucopyranoside into *p*-nitrophenol at pH = 8 for 30 min, the absorbance was measured at 410 nm after heating in boiling water for 3 min. Thus, IU of α-glucosidase was defined as the amount of mM *p*-nitrophenol produced in 1 h. Iodonitrotetrazolium violet (INT) was used as the reaction substrate, and 37 % formaldehyde was used as the reaction terminator to detect DHA [27]. The reduced product of INT was used for calibration. One enzyme unit (EU) was defined as 1 mM INT-depleted per hour of production. The enzyme activity was biomass divided by the unit of activity, by dividing the IU and EU by the mg MLVSS utilised in the enzyme tests, the specific enzyme activities were computed and expressed as enzyme activity per unit biomass.

ACK and coenzyme F₄₂₀ activities were determined and calculated using a UV spectrophotometer and kits [31]. By connecting the oxidation of NADH to NAD⁺ and the conversion of ATP to ADP, the hydroxamate assay was used to measure ACK. The enzyme and 20 mM acetyl phosphate in the sample were mixed and reacted at 37 °C for 3 min and the absorbance at 340 nm was measured. Similarly, the coenzyme F₄₂₀ sample was centrifuged three times and then reconstituted in 30 mL of distilled water before being heated for 30 min at 95 °C in a water bath. After the sample had cooled, it was centrifuged at 12000 × g for 20 min, and the supernatant was precipitated for 120 min using twice as much ethanol as before. To obtain the supernatant for the measurement of coenzyme F₄₂₀ activity, the supernatant was centrifuged once more (12000 × g for 20 min).

SMA was determined by using a fully automated methane potential test system (Bioprocess Control AMPTS II, Switzerland). The system consists of a fermentation unit, an adsorption unit, a gas determination unit, and a main control system connected to a computer for real-time monitoring. In each group of experiments, a mixture of UASB bottom sludge and influent totalling 500 mL was added to serum bottle 1 (B₁) and then sealed and connected to serum bottle 2 (B₂) in the adsorption unit. 100 mL of 3 mol/L NaOH was added to B₂, and a pH indicator was added to ensure that there was no excess of CO₂. Subsequently, the adsorption unit was connected to a gas measurement device monitored by a computer. The temperature was controlled at 25 °C throughout the experiment.

2.5. Data analysis

COD removal efficiency was defined as follow:

$$\text{COD removal efficiency} = \frac{\text{COD}_{\text{influent}} - \text{COD}_{\text{permeate}}}{\text{COD}_{\text{influent}}} \times 100\% \quad (1)$$

where COD_{influent} represents influent COD concentration and COD_{permeate} represents permeate COD concentration.

Mancozeb removal efficiency was defined as follow:

$$\text{Mancozeb removal efficiency} = \frac{\text{Mancozeb}_{\text{influent}} - \text{Mancozeb}_{\text{permeate}}}{\text{Mancozeb}_{\text{influent}}} \times 100\% \quad (2)$$

where Mancozeb_{influent} represents influent mancozeb concentration and Mancozeb_{permeate} represents permeate mancozeb concentration. Moreover, mancozeb can generate ETU through hydrolysis. The definition of influent ETU concentration does not include potential ETU generated by mancozeb. So, the negative removal occurred when more ETU was generated due to mancozeb decomposition than were digested.

ETU removal efficiency was defined as follow:

$$\text{ETU removal efficiency} = \frac{\text{ETU}_{\text{influent}} - \text{ETU}_{\text{permeate}}}{\text{ETU}_{\text{influent}}} \times 100\% \quad (3)$$

where ETU_{influent} represents influent ETU concentration and ETU_{permeate} represents permeate ETU concentration.

Mn²⁺ removal efficiency was defined as follow:

$$\text{Mn}^{2+} \text{ removal efficiency} = \frac{\text{Mn}^{2+}_{\text{influent}} - \text{Mn}^{2+}_{\text{permeate}}}{\text{Mn}^{2+}_{\text{influent}}} \times 100\% \quad (4)$$

where Mn²⁺_{influent} represents influent Mn²⁺ concentration and Mn²⁺_{permeate} represents permeate Mn²⁺ concentration.

Zn²⁺ removal efficiency was defined as follow:

$$\text{Zn}^{2+} \text{ removal efficiency} = \frac{\text{Zn}^{2+}_{\text{influent}} - \text{Zn}^{2+}_{\text{permeate}}}{\text{Zn}^{2+}_{\text{influent}}} \times 100\% \quad (5)$$

where Zn²⁺_{influent} represents influent Zn²⁺ concentration and Zn²⁺_{permeate} represents permeate Zn²⁺ concentration.

SMY was calculated as follows:

$$\text{SMY} = \frac{\text{MC} \times \text{BP}}{\text{Q} \times (\text{COD}_{\text{influent}} - \text{COD}_{\text{permeate}})} \quad (6)$$

where MC represents methane content (%) and BP represents biogas production (mL/d). Q represents the flow (L/d) of the influent.

Analysis of adsorption test were provided in Text S2 of the Supplementary materials.

The t-tests, fitted curves, and fit R² were implemented using the SciPy library in Python 3.12.

3. Results and discussion

3.1. Performance of COD removal efficiency under different HRTs

As illustrated in Fig. 2, the COD removal efficiencies of MTB-assisted AnMBR were usually higher than c-AnMBR in the whole operation time. During stage 1, the permeate COD concentration of R₂ ranged from 793 to 1942 mg/L and that of R₁ ranged from 1102 to 1821 mg/L, which showed a relatively minor difference ($p = 0.14$) between the two reactors. It demonstrates that the COD removal efficiencies were similar for both R₁ and R₂ at HRT of 60 h. There were some notable observations: when the influent COD concentration increased rapidly from 5884 to 8661 mg/L (19 to 23 d), COD removal efficiencies of R₂ and R₁ increased from 78.9 % to 87.0 % and from 74.9 % to 83.4 %, respectively. Moreover, when the influent COD concentration quickly decreased from 5942 to 3723 mg/L (34 to 38 d), the COD removal efficiencies of R₂ and R₁ decreased from 79.5 % to 78.7 % and from 75.7 % to 70.4 %, respectively. Due to the relatively low influent COD concentration, a positive correlation was found between the removal efficiency and influent concentration of COD.

Unfortunately, an electrical issue from 56 to 61 d led to a 5 °C temperature drop,

which resulted in a decrease in removal efficiency from 79.9 % to

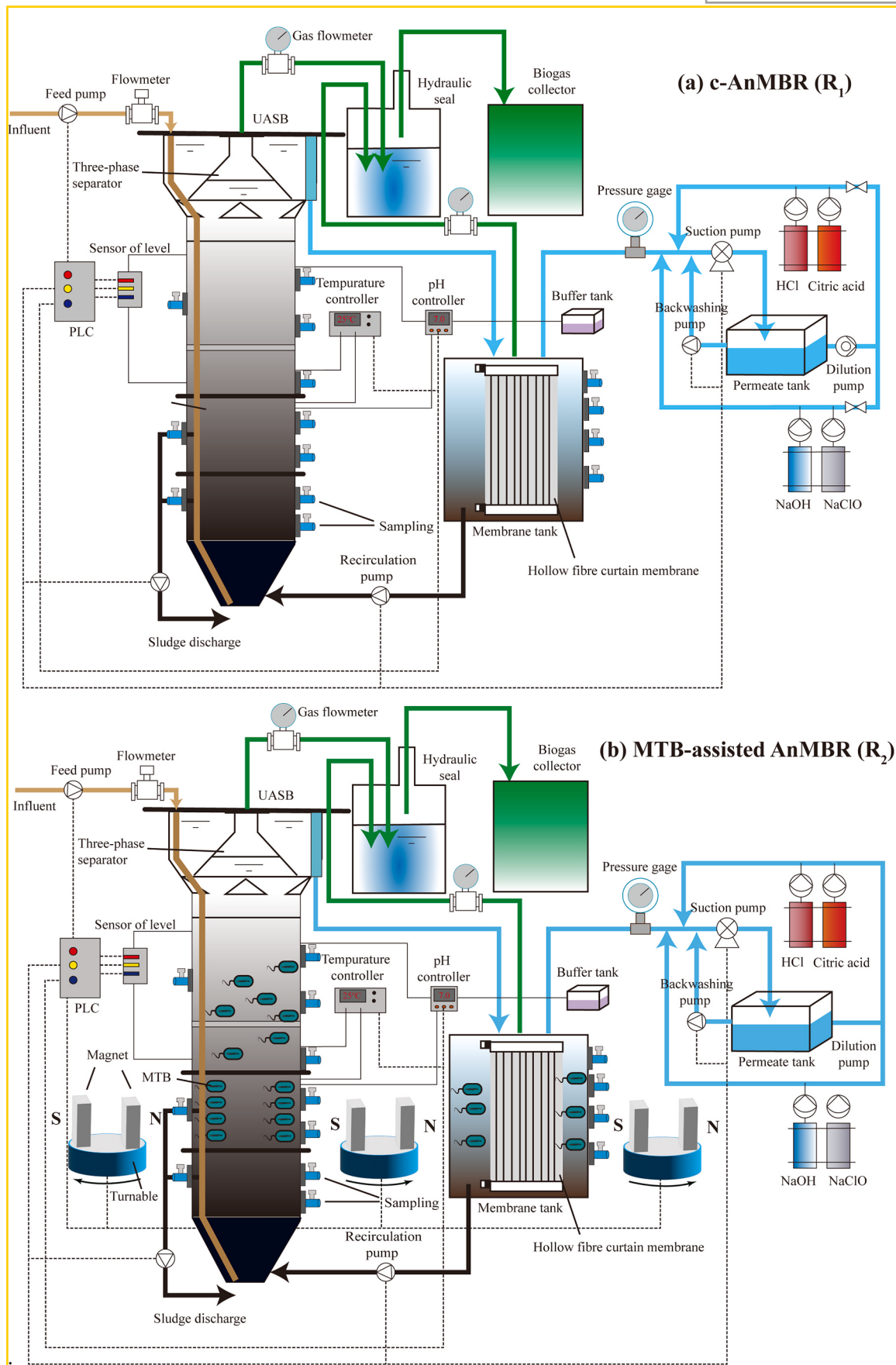


Fig. 1. Process diagrams: (a) conventional anaerobic membrane bioreactor (c-AnMBR); (b) magnetotactic bacteria-assisted AnMBR (MTB-assisted AnMBR).

Table 2

Operating conditions of c-AnMBR and MTB-assisted AnMBR.

Stage	1	2	3	4
Operation period (d)	1–65	66–216	217–280	281–330
HRT (h)	60	48	36	24
Influent COD (mg/L)	3273–8661	6181–18623	3414–7888	6161–8255
OLR (kg COD/(m ³ ·d))	2.5 ± 0.4	4.9 ± 1.4	3.9 ± 1.1	7.5 ± 0.6
Flow rate (L/d)	0.88	1.1	1.47	2.2
Temperature (°C)	25 ± 1	25 ± 1	25 ± 1	25 ± 1
Upflow velocity (m/h)	0.47	0.58	0.78	1.17
Membrane flux (L/(m ² ·h))	8	10	13	20

67.9 % for R₂, and from 78.7 % to 70.0 % for R₁. However, the COD removal efficiency of R₂ subsequently recovered to 79.1 %, while that of R₁ further decreased to 75.2 %. After that, following the shock of high-concentration pollutants in stage 2 (influent COD = 18000 mg/L), the COD removal efficiency of R₁ dramatically decreased from 73.2 % to 48.7 % and that of R₂ decreased from 77.0 % to 65.2 %, respectively (Fig. 2a). At that time, the permeate COD of R₂ was 48.5 % lower than that of R₁. To counteract the effects of high pollutant concentrations on the performance of the two reactors, a strategy was implemented. This strategy involved diluting the influent to a reduced concentration and then incrementally restoring it to the original concentration. Two periods, before and after the shock and dilution, were selected to assess the recovery performance of the two reactors under the shock. The influent COD concentrations in 101–113 d (before shock and dilution) and 169–181 d (after shock and dilution) were 11176 ± 102 mg/L and 11350 ± 198 mg/L, respectively ($p > 0.05$). In 101–113 d, the permeate COD concentration of R₁ was 2372 ± 101 mg/L, which was marginally higher than that of R₂ (2300 ± 45 mg/L), with the difference being not statistically significant ($p = 0.41$). However, in 169–181 d, the permeate COD concentration of R₁ increased to 2756 ± 68 mg/L, while that of reactor R₂ decreased to 1928 ± 167 mg/L, with a pronounced difference observed ($p = 0.001$). These results suggest that the incorporation of MTB could enhance the load resistance of AnMBR under shock conditions.

From 217 to 240 d (stage 3) the average permeate COD concentration of R₂ was 1900 ± 256 mg/L and that of R₁ was 2458 ± 119 mg/L. From 240 to 270 d, the influent COD concentration decreased to about 3000 mg/L; the permeate COD of R₂ reached 783 mg/L, the lowest in all stages. However, when HRT changed to 24 h on 281 d (stage 4), the removal efficiencies of the two reactors dramatically dropped to 66.0 % (R₁) and 65.5 % (R₂), respectively. It could be ascribed to the short contact time between microorganisms and pollutants in both reactors as induced by the short HRT in stage 4.

As shown in Fig. 2b, the average COD removal efficiencies of R₂ at different stages were 78.0 ± 4.8 %, 77.3 ± 2.4 %, 74.6 ± 2.1 % and 59.1 ± 4.4 %, and those of R₁ were 75.5 ± 4.0 %, 74.3 ± 6.2 %, 68.0 ± 5.2 % and 59.2 ± 4.8 %, respectively. In stage 1, there were no statistically significant differences in COD removal efficiencies between R₁ and R₂ ($p = 0.14$). In stage 2, a significant difference was observed ($p = 0.02$). In stage 3, an extremely significant difference was noted ($p < 0.001$). Conversely, in stage 4, there were no statistically significant differences ($p = 0.96$). The median values of R₁ permeate COD concentration were 1444, 2090, 2112 and 2971 mg/L, and those of R₂ were 1242, 2064, 1573 and 3060.5 mg/L, respectively (Fig. 2c). In summary, the COD removal efficiencies of R₁ and R₂ were comparable at HRT of 60 h. R₂ demonstrated a higher removal efficiency at HRT of 48 h (prior to the shock of high concentration pollutants). Conversely, after the shock of high concentration pollutants and HRT of 36 h, the removal efficiency of R₁ was significantly lower than that of R₂. The results obtained suggested that MTB could weaken the negative effect of HRTs decreasing and enhance the load resistance of AnMBR, which could maintain the 65.2 % removal efficiencies under the shock of over 18000 mg/L COD concentration. The reasons could be attributed to that MTB moved along

the magnetic field which promoted sludge contact with pollutants and absorption of toxic pollutants, which could advance the activities of microorganisms and the hydrolysis process in the reactor.

3.2. Promotion of degradation of mancozeb and ETU by MTB

The variations of mancozeb and ETU concentrations in influent and permeate, as well as removal efficiencies, are demonstrated in Fig. 3. The influent mancozeb concentration was greatly high at an average of 4160 ± 712 mg/L. No evident change in permeate concentrations of mancozeb and ETU affected by variations of HRT was observed in the first 280 days (stage 1 to stage 3). On the contrary, when HRT changed to 24 h (stage 4), mancozeb and ETU removal efficiencies of both R₁ and R₂ decreased significantly, which might result from shorter contact time between pollutant and sludge and higher pollutant loading rate. Specifically, the average concentrations of permeate mancozeb of R₁ were over 1000 mg/L, whereas that of R₂ reached less than 600 mg/L when HRT decreased from 60 h to 36 h (stage 1 to stage 3). In stage 4 (HRT of 24 h), the average permeate mancozeb of R₂ was reduced by 51.6 % compared with R₁ which was 2243 mg/L. Additionally, average ETU removal efficiencies of R₁ were 48.82 ± 6.17 %, 27.44 ± 11.32 %, 40.37 ± 4.73 % and 27.73 ± 3.37 % and those of R₂ were 73.01 ± 2.54 %, 58.43 ± 7.38 %, 62.12 ± 5.11 % and 35.46 ± 2.59 % for the four stages, respectively. Results indicated that at HRT of 24 h, the ETU removal efficiencies of R₁ and R₂ are not significantly different compared to those at longer HRTs. It is speculated that this might be due to the ETU produced from the hydrolysis of mancozeb in R₂ not having enough time to undergo further hydrolysis before entering the permeate, while the hydrolysis of ETU in R₁ is even slower. This results in high ETU concentrations and low removal efficiencies in the effluent of both R₁ and R₂.

Abnormally, ETU concentrations of R₁ in the permeate of 126 and 130 d (2116 and 2098 mg/L) were higher than that in the influent (2002 and 2050 mg/L), simultaneously the ETU removal efficiencies decreased to -5.67 % and -2.35 %. This phenomenon was attributed to the ETU hydrolysis rate being slower than the rate of mancozeb converting to ETU. Conversely, this phenomenon was not observed in R₂ during all operational periods. In conclusion, R₂ has a higher refractory pollutants removal efficiency, that of R₂ was unable to be accomplished by R₁.

Previously, Hwang et al. [32] reported 40–100 % removal efficiency of mancozeb and 100 % removal efficiency of ETU with chlorine and chlorine dioxide treatment, but the initial concentration of mancozeb was only 0.2 mg/L in solution. In contrast, R₂ removed mancozeb incompletely in this study, presumably because organic sulfur pesticide wastewater was more complex and toxic to treat and the concentration of influent mancozeb was humorously higher than in the previous study (> 805 mg/L). However, the results still show that the positive effect of MTB on the degradation of characteristic pollutants was significant in organic sulfur pesticide wastewater by AnMBR. It can be inferred that MTB assisted microorganisms of the reactor in removing more mancozeb and ETU, as well as reducing their toxicity to microorganisms, thereby increasing reactor treatment efficiency.

3.3. Elimination of Mn²⁺ and Zn²⁺ by MTB

Because of their non-biodegradable and accumulative nature, heavy metals are a concern for human and environmental health, as well as causing harm to sewage treatment systems [27]. Mn²⁺ and Zn²⁺ were regarded as the main metal contaminants in organic sulfur pesticide wastewater, based on the Guidelines for Monitoring of Sewage Discharging Units – Pesticide Industrial Wastewater (HJ 987–2018, 2018) prepared by the Ministry of Ecology and Environment of the People's Republic of China.

Mn²⁺ average removal efficiency of R₂ was 73.65 ± 8.41 % for four stages (Fig. 4d), which was substantially higher than that of R₁ of 54.00 ± 10.60 % (Fig. 4b). When the influent Mn²⁺ concentration was 2631

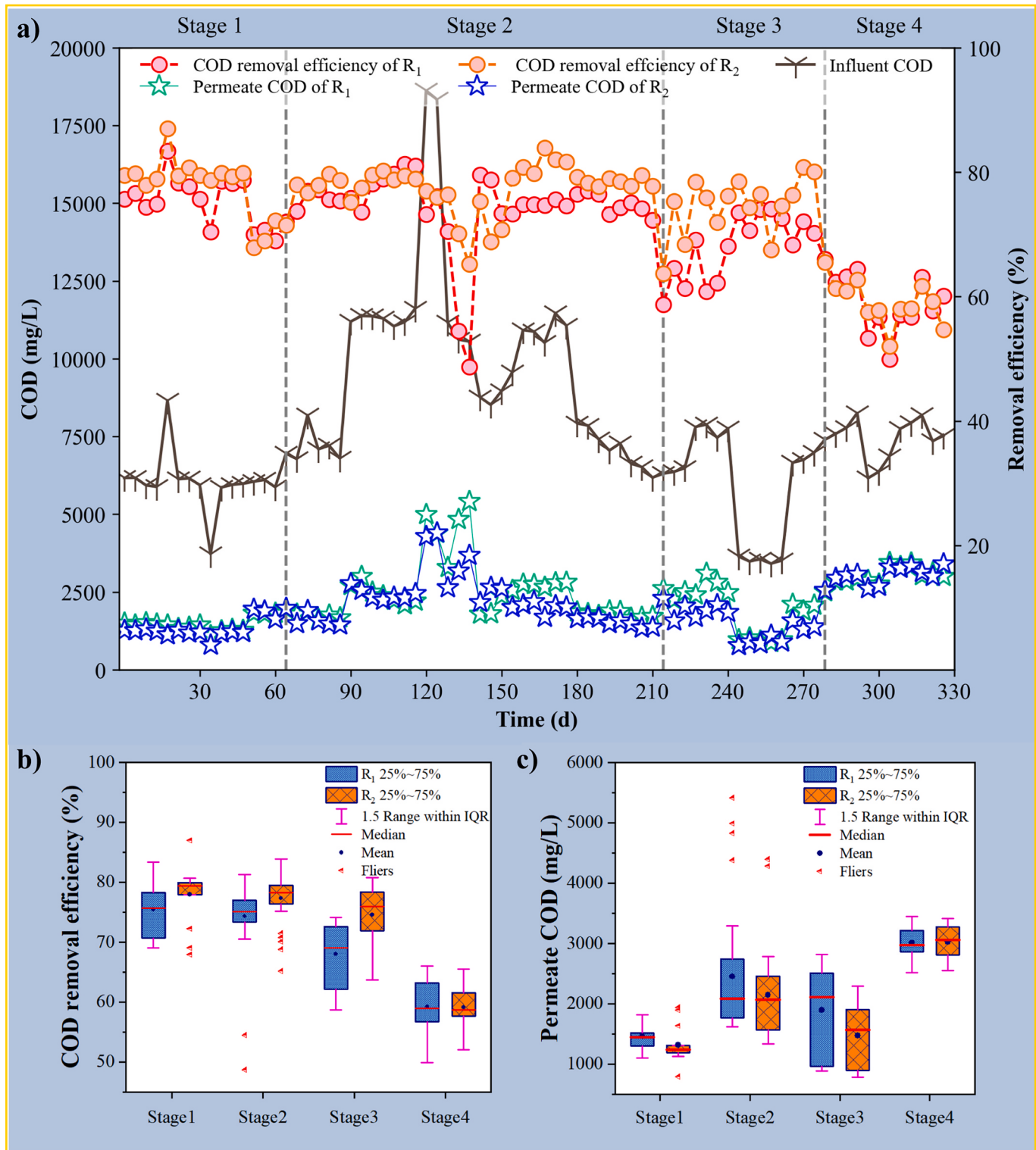


Fig. 2. COD concentration and removal efficiency of R₁ and R₂: (a) variations during the 330 days; (b) distribution of removal efficiencies at different HRTs; (c) distribution of permeate COD concentrations at different HRTs.

mg/L at stage 3, the lowest permeate concentration of R₂ reached 202 mg/L with 92.33 % removal efficiency (Fig. 4c), and that of R₁ was 640 mg/L with 75.69 % removal efficiency, simultaneously (Fig. 4a). Furthermore, the lowest Mn²⁺ removal efficiency of R₂ during stage 4 decreased to 60.83 %, and removal efficiency of R₁ even decreased to only 43.63 %. The high average influent Mn²⁺ concentration (3872 ± 691 mg/L) was encountered, resulting in low removal efficiency,

especially with the short HRT. Previous research has established that the average removal efficiency of Mn²⁺ in groundwater could be 15.26 % through enriched MTB solution [21]. Furthermore, bacterial communities are negatively influenced by Mn²⁺ [33]. These results suggest that MTB may have enhanced the treatment of Mn²⁺ by directly adsorbing and by promoting the activity of other microorganisms, thereby improving the permeate quality and further enhancing the performance

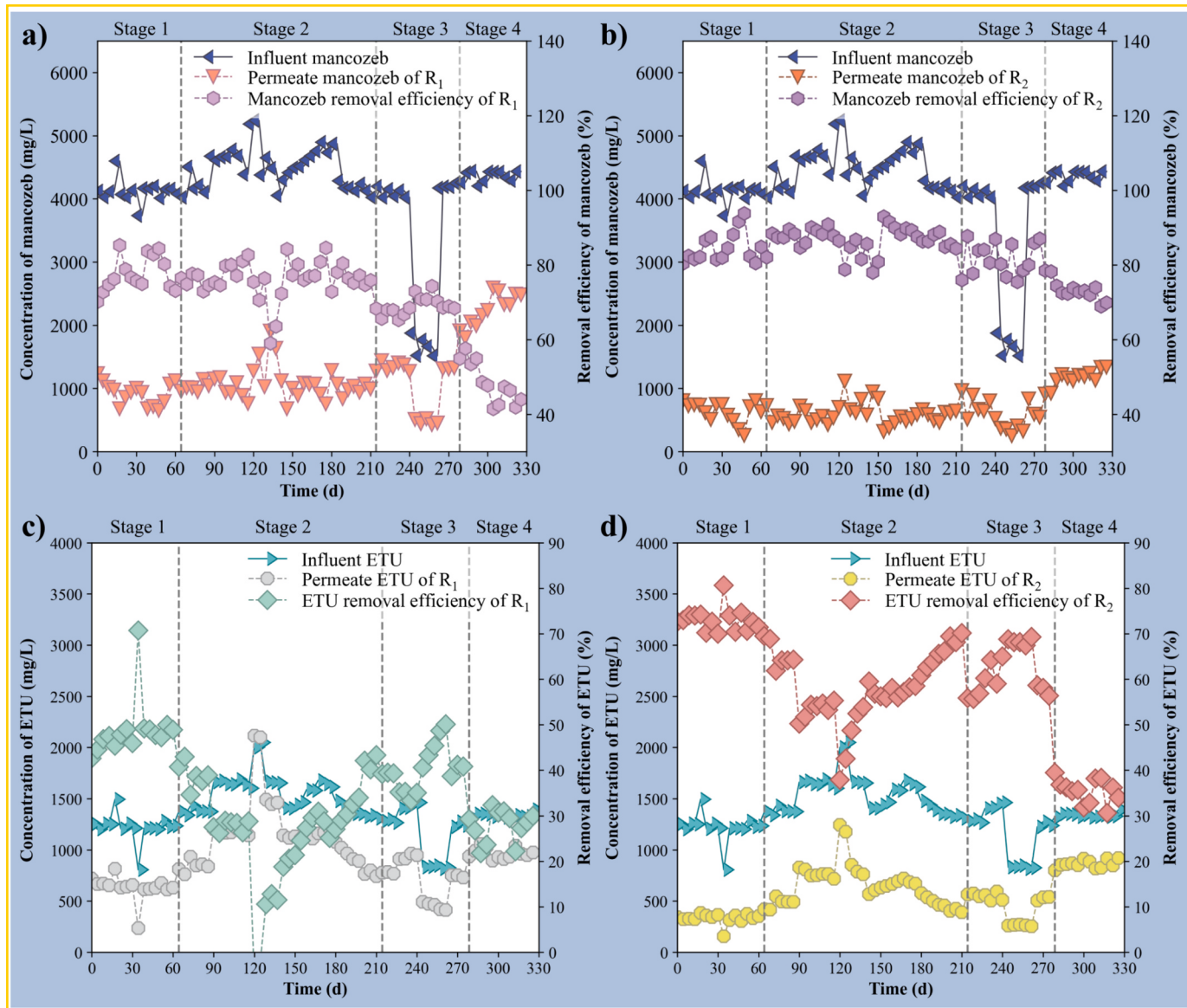


Fig. 3. Changes of mancozeb and ETU concentration and removal efficiency of R₁ and R₂ during operating time: (a) mancozeb of R₁; (b) mancozeb of R₂; (c) ETU of R₁; (d) ETU of R₂.

of the bioreactor.

Fig. 3e-h displays the removal efficiency of Zn²⁺, with median values of 82.56 % and 90.48 % for R₁ and R₂, respectively. In particular, the best Zn²⁺ removal efficiency of R₂ was 99.03 % and removal efficiency of R₁ was 88.60 % at HRT of 36 h. Compared with the average influent Mn²⁺ concentration, Zn²⁺ concentration was too low 0.26 ± 0.02 mg/L, thus removal efficiency of Zn²⁺ was generally higher than that of Mn²⁺. HRT variation of R₂ showed an insignificant impact ($p > 0.05$) on Zn²⁺ removal efficiency but that of R₁ showed a significant impact ($p < 0.05$). The above results show that R₂ can basically achieve complete removal efficiency of Zn²⁺ and eliminate heavy metal toxicity enrichment. Within each stage at HRTs of 60, 48 and 36 h, the removal efficiencies of Mn²⁺ and Zn²⁺ in R₂ gradually increased with the extension of the operational time. This may be since the growth of MTB enhances the remove capacity of heavy metals. The enhanced removal of Mn²⁺ and Zn²⁺ by MTB not only further alleviated the heavy metal toxicity in the reactor, but also may have an important impact on enzyme activity [34,35].

Under the condition of four HRTs, the MTB-assisted AnMBR demonstrated superior performance in Mn²⁺ adsorption, characterized

by lower equilibrium concentrations and higher adsorption capacities (Fig. S1). The maximum adsorption of R₂ occurred at HRT of 48 h, reaching 136 mg/g VSS, which was 21 mg/g VSS higher than the adsorption at HRT of 60 h (Fig. S1b). This suggests that longer HRTs did not necessarily enhance Mn²⁺ adsorption in this study. The removal efficiencies of Zn²⁺ did not significantly differ ($p > 0.05$) between the two reactors under the condition of four HRTs. Furthermore, the adsorption process was characterized using both the Freundlich and Langmuir adsorption models (Table S3 and S4). The results indicated that for R₂, the adsorption process was well-described by Freundlich and Langmuir adsorption models only at HRT of 24 h ($R^2 = 0.8624$ and $R^2 = 0.8830$, respectively), while it could not be described by R₁ and at the other three HRTs ($R^2 < 0.3280$ and $R^2 < 0.3504$). This observation might be attributed to the fact that Mn²⁺ and Zn²⁺ removal involves more than mere molecular-level adsorption. The increased heterogeneity of organic components and the presence of multiple interactive species may diminish the predictive accuracy of the Langmuir isotherm, particularly in unconventional scenarios where adsorption is not limited to a single molecular layer [36]. Nevertheless, the higher fitting coefficients for R₂ compared to R₁ at equivalent stages suggest that the

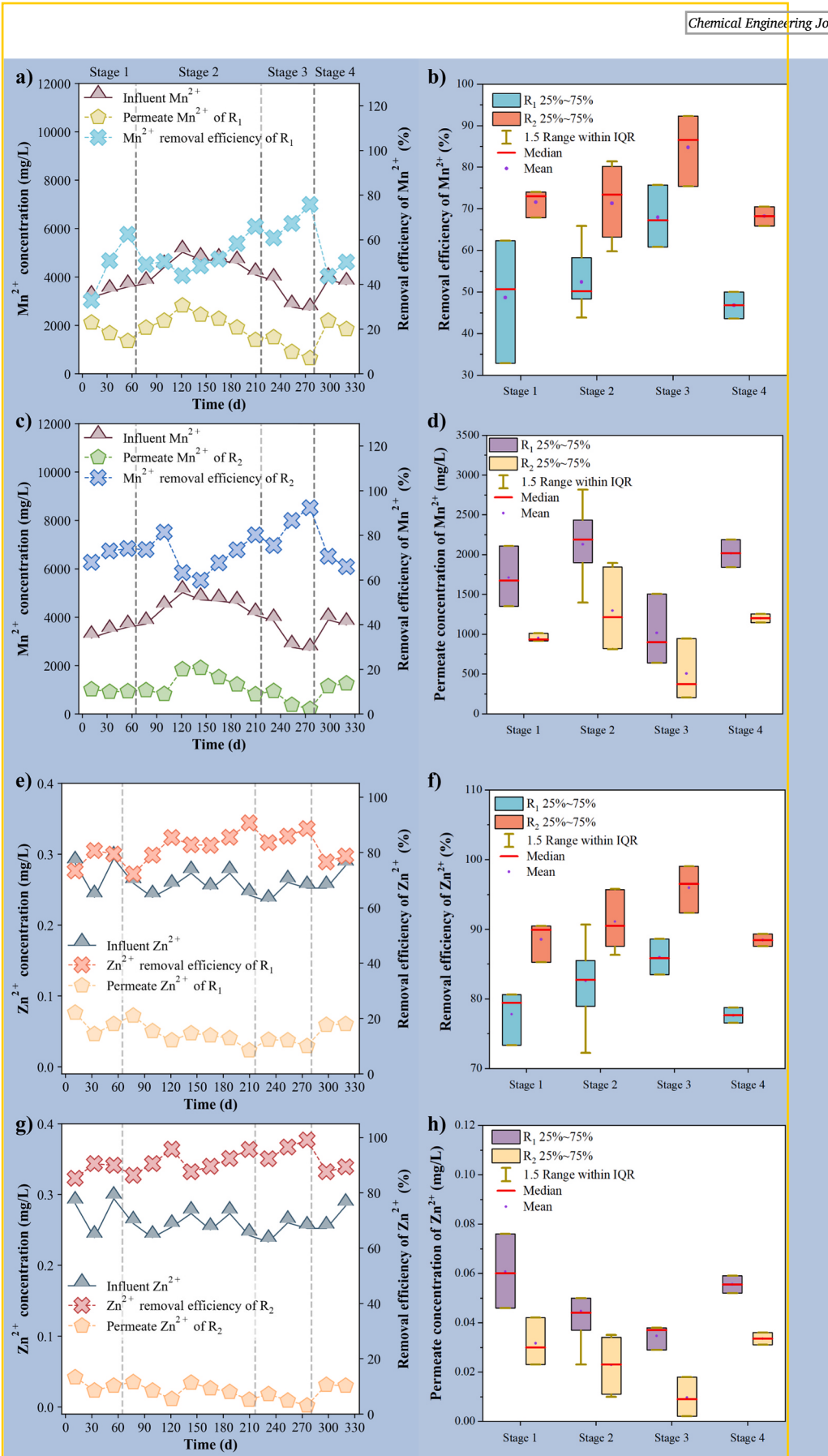


Fig. 4. Comparison of Mn^{2+} and Zn^{2+} concentration and removal efficiency of R_1 and R_2 : (a) Mn^{2+} of R_1 ; (b) Comparison of Mn^{2+} removal efficiency; (c) Mn^{2+} of R_2 ; (d) Comparison of permeate concentration of Mn^{2+} ; (e) Zn^{2+} of R_1 ; (f) Comparison of Zn^{2+} removal efficiency; (g) Zn^{2+} of R_2 ; (h) Comparison of permeate concentration of Zn^{2+} .

incorporation of MTB positively influences the adsorption process.

3.4. Comparison of biogas production and methane content

Conventional AnMBRs encountered suboptimal biogas production and methane content [37]. Biogas productions of R₁ and R₂ are shown in Fig. 5a-b, respectively. The average biogas production of R₁ and R₂ were 1209.05 ± 658.28 mL/d and 1459.77 ± 808.38 mL/d, respectively. As depicted in Fig. 5b, on 130 d, R₂ achieved a maximum biogas production that was 544 mL/d higher than that of R₁ (3425 mL/d). This could be due to the high COD in influent, which provided more organic substances for acetoclastic methanogens and hydrogenotrophic methanogens to digest. Balcioğlu et al. [38] also discovered the production of biogas rose as the concentration of COD rose from 2500 to 18000 mg/L. However, high-concentration pollutants also contain more toxic

substances, which could affect the activities of acetoclastic methanogens and hydrogenotrophic methanogens. Consequently, biogas productions of R₁ and R₂ dropped to 932 and 1467 mL/d on 147d and then gradually recovered to 2322 and 2690 mL/d on 193d, which was similar to the trend of COD removal efficiency (Section 3.1). In addition, biogas productions of R₁ and R₂ were 2053.83 ± 277.47 mL/d and 2604.75 ± 223.91 mL/d, respectively, with an 11000 mg/L influent COD concentration. The biogas production of R₂ at this stage was 26.8 % higher than that of R₁. Electrical problems and pH decreasing also affected negatively biogas production. Previous studies indicated that HRT had a significant effect on biogas production [39], however, in this study, the main factor affecting biogas production in both reactors appear to be the influent COD concentration. Under the same influent conditions, R₂ produced more biogas than R₁ because it removed more pollutants that affect the activity of methanogenic microorganisms.

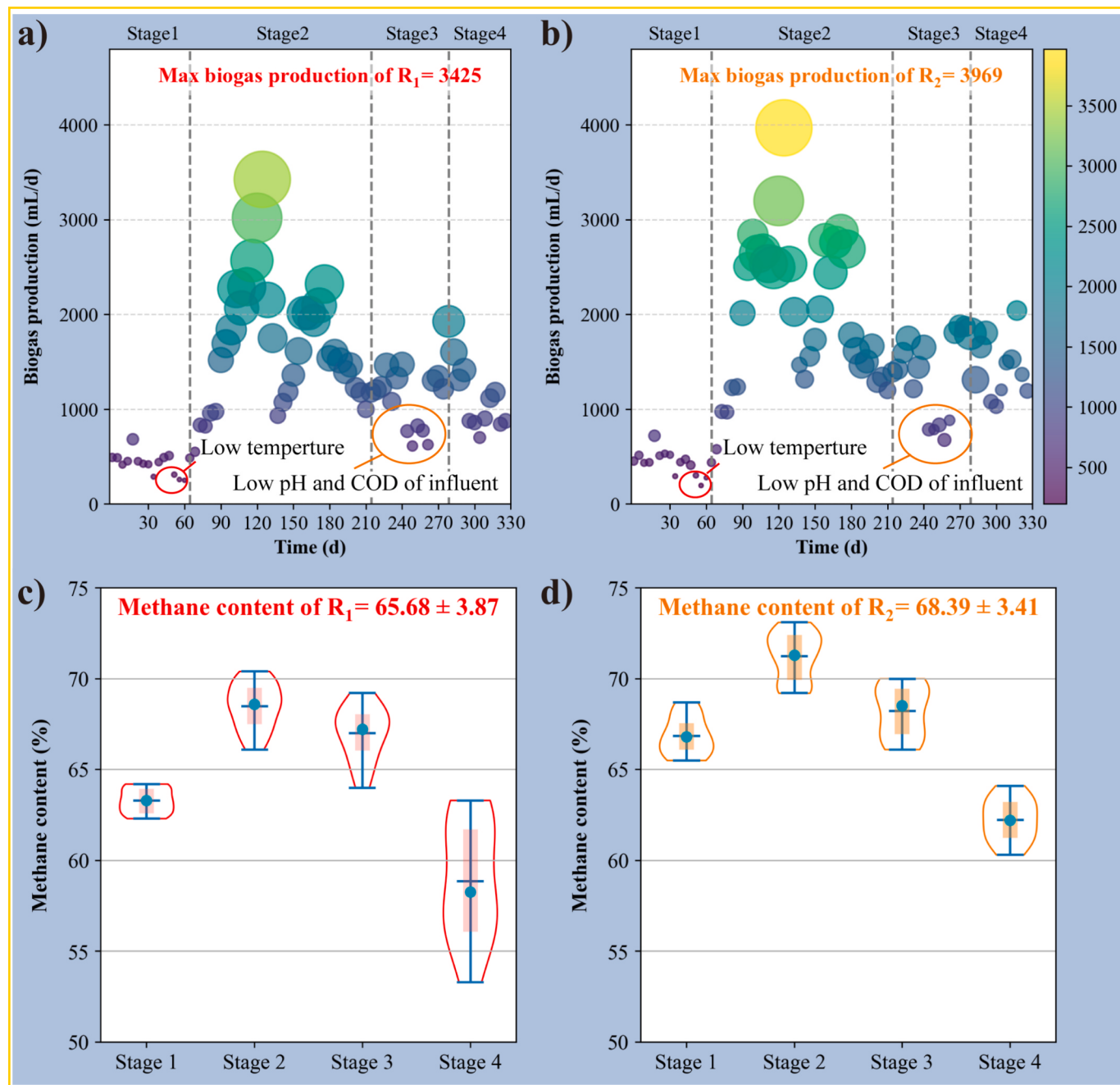


Fig. 5. Characteristic of the biogas production and methane content: (a) Biogas production of R₁; (b) Biogas production of R₂; (c) Methane content of R₁; (d) Methane content of R₂.

The distributions of methane content for each stage of R₁ and R₂ are provided in Fig. 5c-d. The average content for each stage of R₁ was 63.31 ± 0.75 %, 68.59 ± 1.26 %, 67.06 ± 1.44 % and 58.90 ± 3.15 %, and that of R₂ was 66.88 ± 1.03 %, 71.20 ± 1.31 %, 68.25 ± 1.49 % and 62.24 ± 1.10 %. These results inferred that the impact of MTB on the methane content in stage 3 and stage 4 ($p = 0.029$ and $p = 0.003$) is slightly less significant, while it has an extremely significant impact in stage 1 and stage 2 (both $p < 0.001$). Overall, the methane content in the biogas produced by R₂ was higher and more concentrated, reaching a maximum of 73.1 %. The methane content of R₂ was still over 60 % at HRT of 24 h, while the median value of R₁ methane content under the same conditions was only 58.2 %. Compared to R₁, the higher methane content in R₂ indicated that MTB has improved the performance of AnMBR and increased energy recovery potential from organic sulfur pesticide wastewater [40].

3.5. Characterization of SMY and SMA

Fig. 6 demonstrates SMY and SMA variations during the four stages of R₁ and R₂. SMY, defined as the volume of methane produced per gram of COD removed, is a metric that reflects the efficiency of methane production in both reactors. The SMY of R₁ increased from 0.081 L/g-COD_{removed} to 0.228 L/g-COD_{removed} and that of R₂ from 0.080 L/g-COD_{removed} to 0.247 L/g-COD_{removed} in stage 1 and 2, respectively. The low SMY in stage 1 could be attributed to the methanogenic bacteria not adapting to the wastewater conditions. When HRT was decreased to 24 h (stage 4), the SMY decreased to 0.051 L/g-COD_{removed} and 0.089 L/g-COD_{removed}. The tendency was similar to the study of Hu et al. [9], where SMY increased from stage 1 to stage 3 and subsequently decreased from stage 3 to stage 4, indicating short HRT affected AnMBR performance negatively. Above all, the SMY averaged over the whole process of R₂ was 0.149 ± 0.050 L/g-COD_{removed} and that of R₁ was 0.129 ± 0.045 L/g-COD_{removed}. As far as we know, every 1 g of methane production is

theoretically necessary to digest 4 g of COD, and the volume of methane was approximately 1.5 L under standard conditions [41]. Therefore, the theoretical SMY was 0.375 L/g-COD_{removed}, almost impossible to achieve in the experimentation. Compared with other results, Xu et al. [42] utilised an AnMBR with a facultative quorum sensing consortium to achieve the SMY of 0.130 ± 0.050 L/g-COD_{removed} in the treatment of domestic wastewater. The increase of SMY indicates that the higher methane (biogas) production of R₂ was not only due to the digestion of more COD but also because the addition of MTB has enhanced the activity of methanogenic microorganisms.

SMA was determined after extracting the sludge from the bottom of the reactor to determine methanogenic activity at different HRTs [43]. It could be seen that the SMA of R₂ in stage 2 (0.209 g-COD/(g-MLVSS·d)) was 13.9 % higher than that of R₁ (0.180 g-COD/(g-MLVSS·d)), whereas the SMA between R₁ and R₂ was determined to be statistically insignificant in stage 1 ($p = 0.88$) and stage 4 ($p = 0.97$). Compared with other results, the SMA value in a typical UASB was 0.12 g-COD/(g-MLVSS·d) [41]. This suggested that MTB significantly boosted the methanogenic potential of microorganisms in the AnMBR.

3.6. Analysis of enzyme activities

As an essential index for characterizing reactor performance, enzyme activities of protease, α -glucosidase, DHA, ACK and coenzyme F₄₂₀ in four stages are shown in Table 3. Two common hydrolytic enzymes found in AnMBR were protease and α -glucosidase, which could improve the hydrolysis of proteins and polysaccharides, respectively [44]. Compared to the R₁, the activity of protease in stages 1 to 4 increased by 80.6 ± 12.5 %, 79.8 ± 9.6 %, 105.4 ± 23.6 % and 1.2 ± 0.9 %, respectively. Meanwhile, α -glucosidase activity increased by 30.5 ± 2.6 %, 25.7 ± 2.1 %, 21.3 ± 1.1 % and 5.6 ± 0.7 %, respectively (Fig. 7). When HRT was reduced from 36 to 24 h, there were extremely significant differences in both protease and α -glucosidase activities between

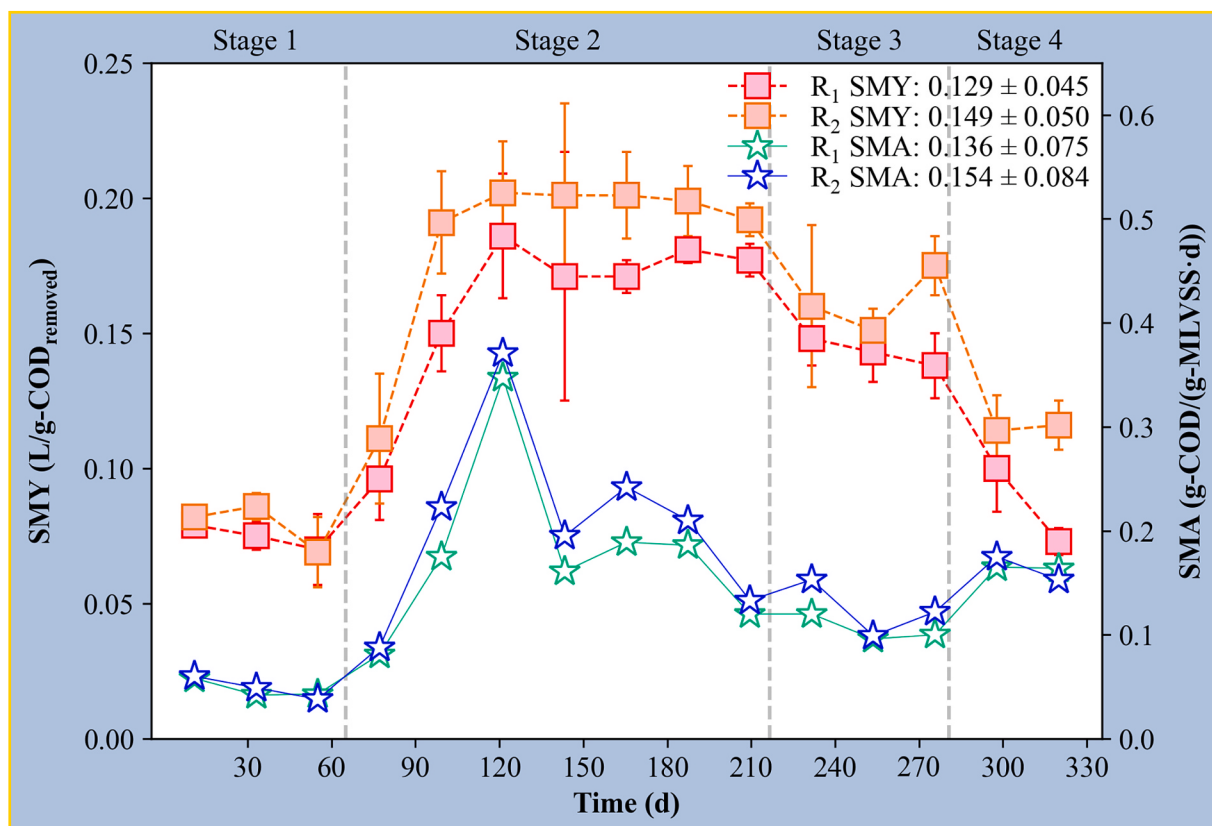


Fig. 6. Specific methane yield and specific methane activity profile.

Table 3Protease, α -glucosidase, DHA, ACK and coenzyme F₄₂₀ activities.

Enzyme activities	Reactors	Stages			
		Stage 1	Stage 2	Stage 3	Stage 4
Protease (IU/g)	R ₁	0.30	0.28	0.25	0.22
	R ₂	0.54	0.51	0.51	0.22
α -Glucosidase (IU/g)	R ₁	0.36	0.33	0.29	0.15
	R ₂	0.47	0.42	0.35	0.16
DHA (EU/g)	R ₁	0.22	0.12	0.25	0.13
	R ₂	0.53	0.44	1.03	0.28
ACK (nmol/(min·g VS))	R ₁	91	100	117	83
	R ₂	101	157	166	135
Coenzyme F ₄₂₀ (nmol/g VS)	R ₁	106	469	271	397
	R ₂	107	604	325	391

stages 3 and 4 (both $p < 0.001$), whereas no significant differences were observed between stages 1 and 2 ($p > 0.05$). The results showed that the assistance of MTB significantly improved the hydrolase activity at longer HRTs (HRT of 60, 48 and 36 h), while the enhancement effect was negligible at HRT of 24 h, which was the same as the trend of COD removal efficiency (Fig. 1a). DHA activity affected the process of anaerobic bacteria creating hydrogen through directed fermentation [45]. In addition, the potential to generate acetic acid was indicated by the activity of ACK [46]. Afterwards, methanogenesis requires the coenzyme F₄₂₀ as a redox cofactor [47]. Over the four stages, the DHA activity of R₂ was $239.8 \pm 13.3\%$, $356.9 \pm 34.5\%$, $419.6 \pm 20.6\%$ and $318.4 \pm 10.8\%$ relative to R₁, respectively. The ACK activity of R₂ was

$111.6 \pm 1.5\%$, $159.6 \pm 6.6\%$, $142.5 \pm 4.3\%$ and $169.6 \pm 10.6\%$ relative to R₁, respectively. Furthermore, the activity of coenzyme F₄₂₀ in R₂ was $195.3 \pm 1.2\%$, $171.3 \pm 2.3\%$, $156.6 \pm 0.7\%$ and $174.2 \pm 0.3\%$ relative to R₁, respectively. At the same time, the activities of coenzyme F₄₂₀ increased to $195.3 \pm 1.2\%$, $171.3 \pm 2.3\%$, $156.6 \pm 0.7\%$ and $174.2 \pm 0.3\%$, respectively. As shown in Fig. 7, when HRT was reduced from 60 to 24 h (stage 1 to stage 4), the activity ratios between R₂ and R₁ of DHA, ACK and coenzyme F₄₂₀ did not exhibit a regular pattern ($p < 0.05$). This observation implies that although methanogenic enzyme activity associated with methane production of R₂ is enhanced compared to R₁, this enhancement is not directly proportional to changes in HRT. Previous research suggested that Fe₃O₄ might enhance hydrolytic enzyme activity, hence promoting AD hydrolysis [48]. Similarly, the MTB also contained magnetosomes consisting mainly of high-purity Fe₃O₄, which exerted a positive effect on the hydrolytic enzymes. Furthermore, excessive heavy metal, mancozeb and ETU concentrations may be detrimental to hydrolysis processes, but the assistance of MTB reduces the toxic effects of pollutants, making enzyme activities of R₂ increase compared with R₁.

3.7. Influence of refractory pollutants and heavy metals on enzyme activities

The permeate mancozeb, ETU, Mn²⁺, and Zn²⁺ concentrations respectively concerning the enzyme activities of R₁ and R₂ are shown in Fig. 8. In the two reactors, mancozeb concentration was significantly negatively correlated with the activities of protease ($R^2 = 0.9720$ and $=$

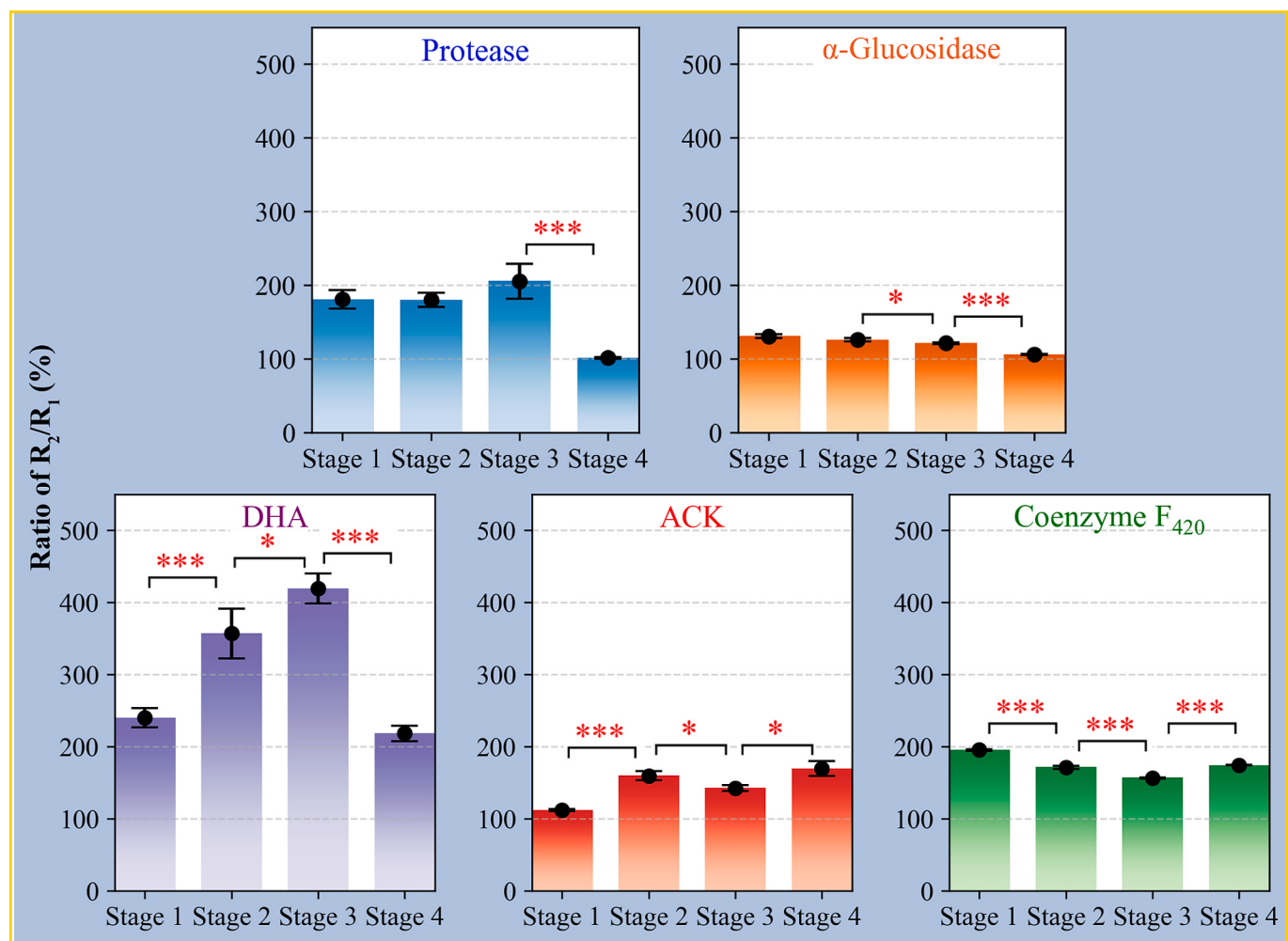


Fig. 7. Ratio of the enzyme activities of R₂ to R₁ (**, ***, mean these two stages are significantly different. ** means, $p < 0.05$; *** means $p < 0.001$).

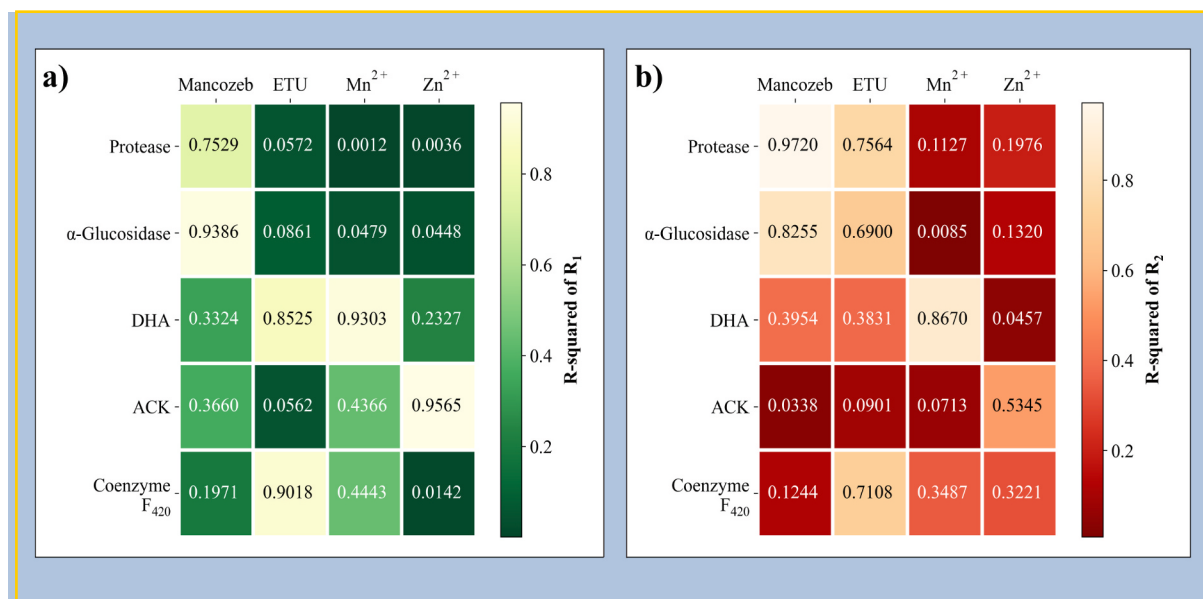


Fig. 8. R-squared heatmap of R_1 and R_2 : (a) R-squared heatmap of R_1 ; (b) R-squared heatmap of R_2 .

0.7529) and α -glucosidase ($R^2 = 0.9386$ and $R^2 = 0.8255$) and also had a weak effect on DHA activity ($R^2 = 0.3324$ and $R^2 = 0.3954$). In addition, the ETU concentration of R_2 is related to the activities of four enzymes except ACK, but that of R_1 only shows a significant correlation only with DHA ($R^2 = 0.8525$) and coenzyme F₄₂₀ ($R^2 = 0.9018$). Among the enzyme activities related to Mn^{2+} , DHA is the most significant with an R^2 of 0.9303 in R_1 and 0.8670 in R_2 . However, only ACK has a significant relationship with the Zn^{2+} of R_1 ($R^2 = 0.9565$) and that of R_2 is weaker ($R^2 = 0.5345$).

The mathematical model of pollutant concentrations and enzyme activities with good correlation is shown in Fig. 9. As shown in Fig. 9a-b, the protease and α -glucosidase activities decreased as the mancozeb concentration increased, indicating that mancozeb significantly inhibited the hydrolase activity and further reduced the COD removal efficiency. The DHA activity of R_2 decreased rapidly with the increase of mancozeb concentration, which indicated that low concentrations of mancozeb could inhibit DHA activity and further affect methane yield (Fig. 9c). Similarly, increased concentrations of ETU also significantly inhibited the activities of protease and DHA (Fig. 9d-e). Paradoxically, coenzyme F₄₂₀ activity was positively correlated with ETU (Fig. 9f). However, when viewed in conjunction with the two reactors, the relatively low ETU concentration of R_2 would not yet have had a substantial effect on coenzyme F₄₂₀ activity. In contrast, the ETU concentration of R_1 was over 1000 and 600 mg/L, respectively, resulting in a coenzyme F₄₂₀ activity that was consistently no higher than 600 nmol/g VS. Conversely, under the same stress conditions, the activity of coenzyme F₄₂₀ in R_2 could exceed 800 nmol/g VS, indicating that the addition of MTB mitigated the toxicity of ETU. Although mancozeb and ETU have a little effect on DHA, the most important factor is Mn^{2+} concentration. DHA activity of R_1 decreased from 0.245 EU/g to 0.122 EU/g in the increase of Mn^{2+} concentration from 300 mg/L to 1409 mg/L (Fig. 9g). Whereas it was evident that the DHA activity of R_1 decreased with increasing Zn^{2+} concentration, and that of R_2 was more sensitive to its increase (Fig. 9i).

3.8. Relationships between enzyme activities, COD removal efficiency, and methane yield

In the anaerobic degradation process, removing COD mainly relies on microbial digestion of biodegradable organic materials, but microorganisms cannot directly metabolize the particulate organic present

and macromolecules (mainly proteins, and polysaccharides) in the organic sulfur pesticide wastewater. Thus, the first step is the hydrolysis of organic matter such as proteins and polysaccharides into amino acids and monosaccharides through the secretion of hydrolytic enzymes by microorganisms. Therefore, the COD removal efficiency may be influenced by the activity of hydrolytic enzymes. The polynomial fitting models of protease and α -glucosidase with COD removal efficiency are illustrated in Fig. 10. The concentration of protease is linearly correlated with the COD removal efficiency in the first order. As shown in Fig. 10a, R_2 up to $R^2 = 0.9972$ and those of R_1 also showed a strong correlation ($R^2 = 0.9590$). This suggested that an increase in protease activity can significantly promote COD removal efficiency. Combined with Sections 3.1 and 3.6, it was reasonable to speculate that MTB promoted the hydrolysis of protein in anaerobic biological treatment by increasing protease activity, which in turn increased COD removal efficiency.

As shown in Fig. 8b, the fitting performances between α -glucosidase activity and COD removal efficiency ($R^2 = 0.7477$ and 0.7413) were slightly lower than those between protease activity and COD removal efficiency ($R^2 = 0.9972$ and 0.9590). When the α -glucosidase activity of R_1 increased from 0.15 to 0.33 IU/g, along with an increase in the COD removal efficiency from 57.8 % to 76.2 %, whereas the COD removal efficiency decreased to 73.3 % when the activity was 0.36 IU/g. A similar situation was observed in R_2 , where the removal efficiency was 75.9 % when the activity was 0.35 IU/g, while when the activity was 0.47 IU/g, the removal efficiency decreased to 73.7 %. This indicated that a further increase in α -glucosidase activity of reactors would not improve COD removal efficiency when the activity reached the critical value between 0.29 and 0.33 IU/g. This could also explain why the α -glucosidase properties of R_2 in Section 3.6 showed a small enhancement (21.3–30.5 %) compared to R_1 . However, the assistance of MTB could make AnMBR reach the critical value at HRT of 36 h, but the c-AnMBR reached it at HRT over 48 h.

ACK, coenzyme F₄₂₀ and DHA are three enzymes related to the methanogenic process, and their partial relationships with the four methanogenic indicators (biogas production, methane content, SMY and SMA) are shown in Fig. 10c-h. The correlation between ACK and SMY of R_2 ($R^2 = 0.8796$) was greater than that of R_1 with $R^2 = 0.4404$ (Fig. 10c). As displayed in Fig. 10d, ACK activity showed a similar relationship with biogas production, with a much stronger fit of R_2 ($R^2 = 0.7082$) than that of R_1 ($R^2 = 0.0458$). ACK directly characterizes the performance of the reactor to produce acetic acid which is an important precursor used

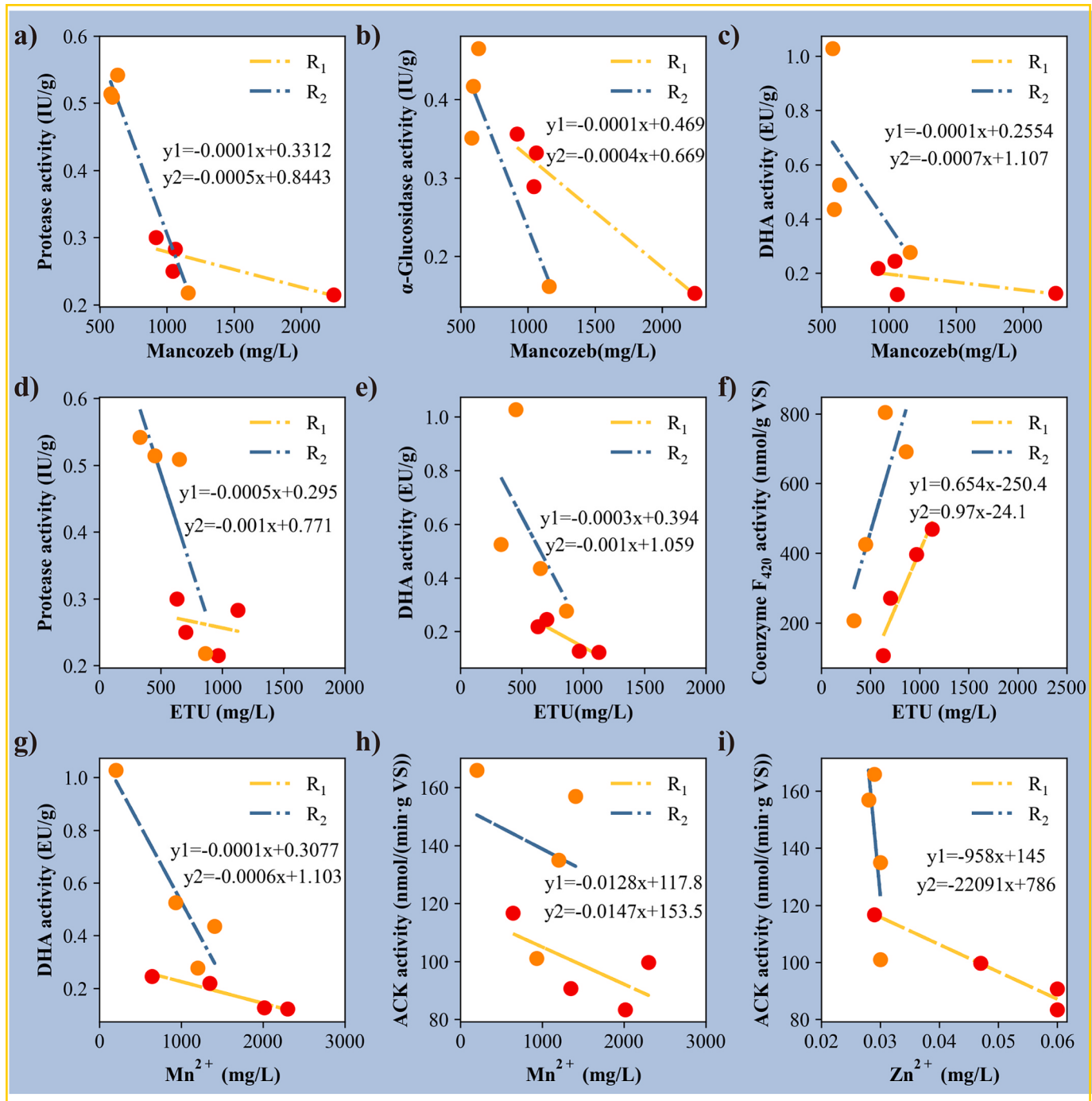


Fig. 9. Correlation model between permeate concentrations of refractory pollutants, heavy metals and enzyme activities. (a) mancozeb – protease; (b) mancozeb – α -glucosidase; (c) mancozeb – DHA; (d) ETU – protease; (e) ETU – DHA; (f) ETU – coenzyme F₄₂₀; (g) Mn²⁺ – DHA; (h) Mn²⁺ – ACK; (i) Zn²⁺ – ACK.

by acetoclastic methanogens for methanogenesis. The lower fit of R₁ would be due to the reactor methanogenic bacteria thoroughly not utilising acetic acid for methane production, resulting in lower SMA and biogas production. On the other hand, the higher fitting performance indicated that the ACK activity had become the limiting factor for the methanogenesis of R₂. The amount of methane (biogas) production is dependent on the amount of acetic acid production. Therefore, the high ACK activity of R₂ improved the methanogenic capacity. There is also a good correlation with biogas for coenzyme F₄₂₀, with 0.9286 and 0.8490 of R₁ and R₂, respectively (Fig. 10e).

In comparison, as shown in Fig. 10f, coenzyme F₄₂₀ demonstrates a stronger correlation with SMA of R₁ and R₂, with $R^2 = 0.9821$ and 0.9638, respectively. Coenzyme F₄₂₀ is usually regarded as an important

indicator for characterizing methanogenic activity in anaerobic processes [49]. The activity of coenzyme F₄₂₀ were increased by the assistance of MTB and further improved biogas production and SMA. Notably, DHA was another enzyme associated with SMA. Nevertheless, DHA activity became negatively correlated with SMA to a higher degree in R₁ ($R^2 = 0.7196$), while the two could be considered unrelated in R₂ ($R^2 = 0.0323$) (Fig. 10g-h). The dehydrogenase activity in the AnMBR represents anaerobic bacteria that produce hydrogen through directed fermentation [45], the anaerobic bacteria which produce hydrogen could lead to substrate competition with acetoclastic methanogens, thus decreasing the SMA of R₁. In contrast, the average SMA of R₂ was 11.7% higher than that of R₁. Among the five enzymes in both reactors, only ACK in R₁ showed a weak correlation with methane content, with a

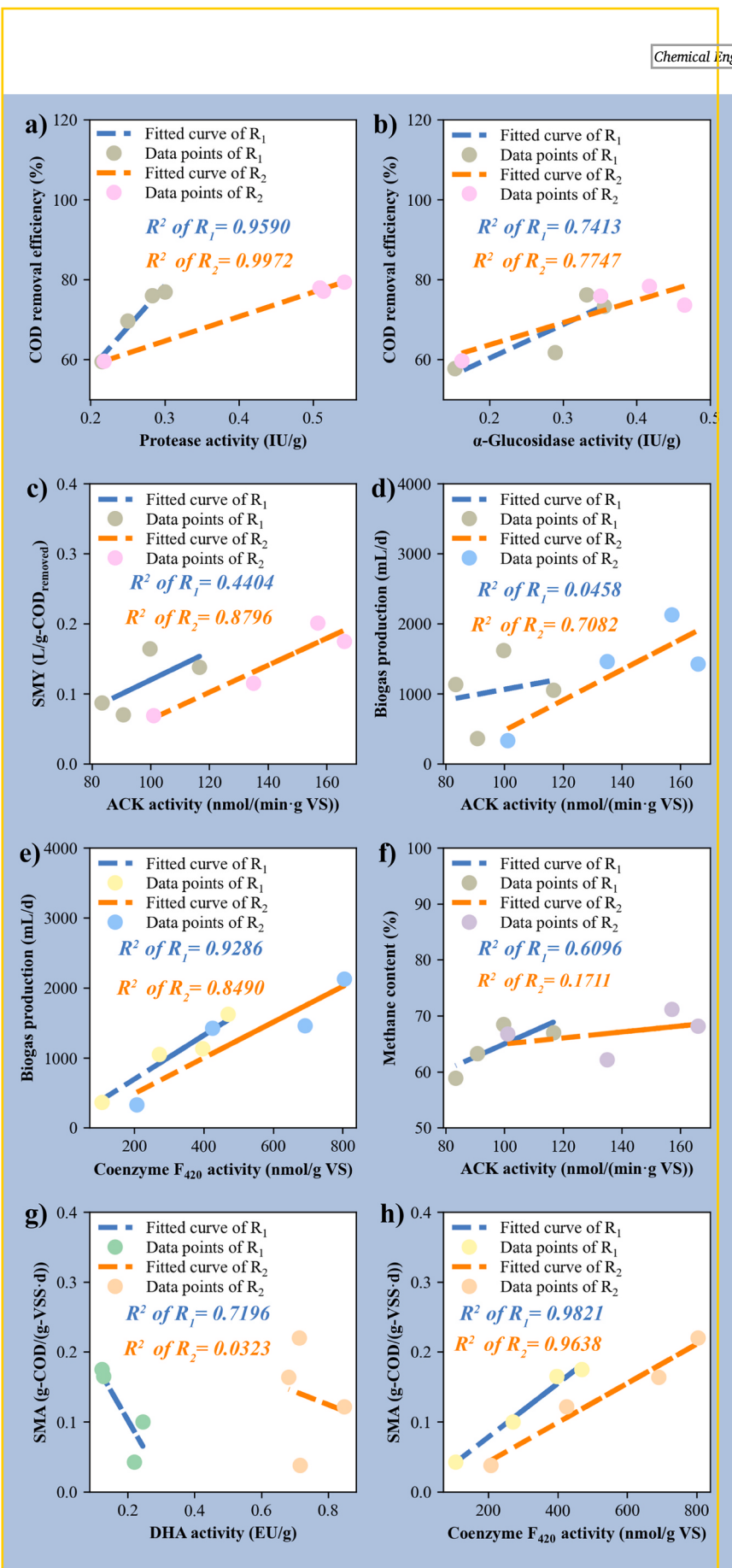


Fig. 10. Fitting curves of enzymes activity, COD removal efficiency and methane yield of R₁ and R₂. (a) protease – COD removal efficiency; (b) α -glucosidase – COD removal efficiency; (c) ACK – SMY; (d) ACK – biogas production; (e) coenzyme F₄₂₀ – biogas production; (f) ACK – methane content; (g) DHA – SMA; (h) coenzyme F₄₂₀ – SMA.

correlation coefficient of $R^2 = 0.6096$. This again verified that acetic acid in R_1 was not fully utilised and the methanogenic performance in biogas was still not optimal, whereas the addition of MTB might alter the distribution and abundance of microbial communities within the reactor, which further increased the methanogenesis-related enzyme activities and finally improved the methanogenic capacity.

The above results showed that mancozeb and ETU in organic sulfur pesticide wastewater had significant inhibitory effects on hydrolases, and had a certain impact on enzymes related to the methanogenesis process. On the other hand, Mn^{2+} and Zn^{2+} inhibited the activity of DHA and ACK, respectively, and further influenced methane yield by reducing the substrate acetic acid required by acetoclastic methanogens and the activity of hydrogen-producing microorganisms [47,50]. As mentioned before, MTB could assist in removing mancozeb and ETU to weaken their toxicity. At the same time, the directional movement of MTB under the magnet field could promote the contact of pollutants with the bottom sludge to increase the enzyme activity, and further improve the COD removal efficiency and methane yield. In addition, MTB had strong adsorption on Mn^{2+} and Zn^{2+} , which reduced the high osmotic pressure due to high Mn^{2+} concentration and the inhibition of Zn^{2+} on biogas production. Although c-AnMBR also had high removal efficiency of Mn^{2+} and Zn^{2+} due to microorganisms stimulated by toxic pollutants and heavy metals to produce extracellular polymers (EPS) and soluble microbial products (SMP), which could complex with metal ions and protect microorganisms from toxicity [27]. However, excessively high EPS reduces the exposure of microorganisms to contaminants and could cause serious membrane fouling. In contrast, MTB mitigated the toxic effects on microorganisms of the AnMBR by removing mancozeb, ETU, Mn^{2+} and Zn^{2+} from the influent, resulting in less secretion of EPS and SMP by microorganisms. Additionally, the applied magnetic field has been shown to attenuate the formation of EPS and SMP in MBR [51]. In summary, the process by which MTB enhances the AnMBR can be outlined as follows: The combined effect of MTB and the enhanced magnetic field reduced the toxic pollutants in the organic sulfur pesticide wastewater, decreased the interference of refractory pollutants such as mancozeb and ETU, and heavy metals like Mn^{2+} and Zn^{2+} on microorganisms. This leads to an increase in the activity of hydrolytic enzymes and methanogenesis-related enzymes, thereby further improving the COD removal efficiency and methane production capability.

4. Conclusion

This study pioneers the integration of MTB into an AnMBR for treating organic sulfur pesticide wastewater. Quantitative analyses revealed that R_2 outperformed R_1 , achieving significantly higher removal efficiencies for mancozeb (20.92 %), ETU (26.81 %), Mn^{2+} (17.64 %), and Zn^{2+} (10.43 %). Concurrently, R_2 exhibited enhanced enzymatic activities: protease (205.4 %), α -glucosidase (130.5 %), dehydrogenase (419.6 %), acetate kinase (169.6 %), and coenzyme F₄₂₀ (128.8 %), with statistically distinct performance across operational stages ($p < 0.05$). These improvements correlated with elevated biogas production (3969 mL/d) and methane content (68.39 ± 3.41 %), yielding a 15.5 % higher specific methane yield and 13.2 % greater specific methane activity than R_1 . Strong interdependencies ($R^2 > 0.7529$) were observed among refractory pollutant degradation, enzymatic activity, COD removal efficiencies, and methane productivity, suggesting that MTB alleviated heavy metal inhibition, thereby improving the efficiencies of AnMBR in treating pollutants. Future research should prioritize in situ magnetosome-mediated mechanisms, analysis of the microbial communities, influencing factors of membrane fouling and techno-economic optimization for scaling MTB-assisted anaerobic systems.

CRediT authorship contribution statement

Shiming Cui: Writing – original draft, Visualization, Validation, Software, Methodology, Investigation, Formal analysis, Data curation, Conceptualization. **Dongxue Hu:** Writing – review & editing, Supervision, Software, Methodology, Funding acquisition, Formal analysis, Conceptualization. **Zhaobo Chen:** Writing – review & editing, Supervision, Project administration, Methodology, Funding acquisition, Conceptualization. **Yifan Wang:** Writing – review & editing, Visualization, Validation, Formal analysis, Data curation, Conceptualization. **Jitao Yan:** Writing – review & editing, Resources, Methodology, Investigation. **Shuya Zhuang:** Supervision, Project administration, Methodology, Data curation. **Bei Jiang:** Writing – review & editing, Supervision, Software. **Hui Ge:** Validation, Supervision. **Zihan Wang:** Writing – review & editing, Visualization, Validation, Formal analysis, Data curation, Conceptualization. **Pengcheng Zhang:** Project administration.

Declaration of competing interest

The authors declare that they have no known competing financial interests or personal relationships that could have appeared to influence the work reported in this paper.

Acknowledgments

This work was supported by the National Natural Science Foundation of China (Nos. 22376021, 22076020 and 51778114); Department of Science & Technology of Liaoning province (2024JH2/102600094); Natural Science Foundation of Liaoning Province (No. 2023-MS-131); Scientific research project of Liaoning Provincial Department of Education (No. LJKZ0020). This work was also supported by the Science and Technology Innovation Fund Project of Dalian (2023JJ13SN072).

Appendix A. Supplementary data

Supplementary data to this article can be found online at <https://doi.org/10.1016/j.cej.2025.161397>.

Data availability

Data will be made available on request.

References

- [1] Ministry of Agriculture and Rural Affairs of the People's Republic of China, the national production of chemical pesticide products (100% active ingredient) of China. <http://zdsxxw.moa.gov.cn:8080/nyb/pc/search.jsp>
- [2] M.V. Cesio, H. Heinzen, Mancozeb, in: P. Wexler (Ed.), Encyclopedia of Toxicology (Fourth Edition), Academic Press, Oxford, 2024, pp. 5–9. <https://doi.org/10.1016/B978-0-12-824315-2.01024-1>
- [3] J. Runkle, J. Flocks, J. Economos, A.I. Dunlop, A systematic review of Mancozeb as a reproductive and developmental hazard, Environ. Int. 99 (2017) 29–42, <https://doi.org/10.1016/j.envint.2016.11.006>
- [4] C.L. Sweeney, Y. Park, D.A. Shea, J.S. Kim, N-nitrosoethylenethiourea formation at environmentally-relevant concentrations of ethylenethiourea in a pooled groundwater sample, Sci. Total Environ. 761 (2021) 143300, <https://doi.org/10.1016/j.scitotenv.2020.143300>
- [5] S. Yang, Q. Wen, Z. Chen, Impacts of Cu and Zn on the performance, microbial community dynamics and resistance genes variations during mesophilic and thermophilic anaerobic digestion of swine manure, Bioresour. Technol. 312 (2020) 123554, <https://doi.org/10.1016/j.biortech.2020.123554>
- [6] K.Y. He, X.C. Guo, G.F. Wang, J.P. Xiong, H.L. Peng, F.Y. Lai, J.B. He, Excellent treatment effect of actual wastewater from a pesticide plant using electro-Fenton process catalyzed by natural pyrite, J. Environ. Chem. Eng. 11 (6) (2023), <https://doi.org/10.1016/j.jece.2023.111211>
- [7] Z.Y. Wang, K.L. Li, J.J. Guo, C.F. Yang, L. Yan, W. Feng, Y. Zhang, J. Wang, Elimination of pesticide from high salinity wastewater by electrochlorination process: Active chlorine species and scale-up performance, Sep. Purif. Technol. 306 (2023), <https://doi.org/10.1016/j.seppur.2022.122572>

- [8] M.H. El-Saeid, M.O. Alotaibi, M. Alshabanat, K. Alharbi, A.S. Altowyan, M. Al-Anazi, Photo-Catalytic Remediation of Pesticides in Wastewater Using UV/TiO₂, Water 13 (21) (2021), <https://doi.org/10.3390/w13213080>.
- [9] D. Hu, L. Liu, W. Liu, L. Yu, J. Dong, F. Han, H. Wang, Z. Chen, H. Ge, B. Jiang, X. Wang, Y. Cui, W. Zhang, Y. Zhang, S. Liu, L. Zhao, Improvement of sludge characteristics and mitigation of membrane fouling in the treatment of pesticide wastewater by electrochemical anaerobic membrane bioreactor, Water Res. 213 (2022) 118153, <https://doi.org/10.1016/j.watres.2022.118153>.
- [10] P.S. Goh, W.J. Lau, A.F. Ismail, Z. Samawati, Y.Y. Liang, D. Kanakaraju, Microalgae-Enabled Wastewater Treatment: A Sustainable Strategy for Bioremediation of Pesticides, Water 15 (1) (2023), <https://doi.org/10.3390/w15010070>.
- [11] L.-L. Zheng, J. Zhang, X.-Z. Liu, L. Tian, Z.-S. Xiong, X. Xiong, P. Chen, D.-S. Wu, J.-P. Zou, Degradation of pesticide wastewater with simultaneous resource recovery via ozonation coupled with anaerobic biochemical technology, Chemosphere 300 (2022) 134520, <https://doi.org/10.1016/j.chemosphere.2022.134520>.
- [12] S. Akinapally, B. Dheeravath, K.K. Pangal, H. Vurimindi, S. Sanaga, Treatment of pesticide intermediate industrial wastewater using hybrid methodologies, Appl. Water Sci. 11 (3) (2021) 56, <https://doi.org/10.1007/s13201-021-01387-4>.
- [13] H. Min, D. Hu, H. Wang, Y. Zhao, Y. Cui, K. Luo, L. Zhang, W. Liu, P. Wu, H. Ge, A. Wang, Y. Zhang, Electrochemical-assisted hydrolysis/acidification-based processes as a cost-effective and efficient system for pesticide wastewater treatment, Chem. Eng. J. 397 (2020) 125417, <https://doi.org/10.1016/j.cej.2020.125417>.
- [14] R. Wang, Z. An, L. Fan, Y. Zhou, X. Su, J. Zhu, Q. Zhang, C. Chen, H. Lin, F. Sun, Effect of quorum quenching on biofouling control and microbial community in membrane bioreactors by *Brucella* sp. ZII, J. Environ. Manag. 339 (2023) 117961, <https://doi.org/10.1016/j.jenvman.2023.117961>.
- [15] L. Liu, W. Liu, L. Yu, J. Dong, F. Han, D. Hu, Z. Chen, H. Ge, B. Jiang, H. Wang, Y. Cui, W. Zhang, X. Zou, Y. Zhang, Optimizing anaerobic technology by using electrochemistry and membrane module for treating pesticide wastewater: Chemical oxygen demand components and fractions distribution, membrane fouling, effluent toxicity and economic analysis, Bioresour. Technol. 346 (2022) 126608, <https://doi.org/10.1016/j.biortech.2021.126608>.
- [16] M. Marmol, E. Gachon, D. Faivre, Colloquium: Magnetotactic bacteria: From flagellar motor to collective effects, RevModPhys. 96 (2) (2024), <https://doi.org/10.1103/RevModPhys.96.021001>.
- [17] X. Wang, Y. Li, J. Zhao, H. Yao, S. Chu, Z. Song, Z. He, W. Zhang, Magnetotactic bacteria: Characteristics and environmental applications, Front. Environ. Sci. Eng. 14 (4) (2020) 56, <https://doi.org/10.1007/s11783-020-1235-z>.
- [18] Q. Li, H. Chen, X. Feng, C. Yu, F. Feng, Y. Choi, P. Lu, T. Song, X. Wang, L. Yao, Nanoparticle-Regulated Semiartificial Magnetotactic Bacteria with Tunable Magnetic Moment and Magnetic Sensitivity, Small 15 (15) (2019) 1900427, <https://doi.org/10.1002/smll.201900427>.
- [19] I. Shen, G.A. Paterson, Y. Wang, J.I. Kirschvink, V. Pan, W. Lin, Renaissance for magnetotactic bacteria in astrobiology, ISME J. 17 (10) (2023) 1526–1534, <https://doi.org/10.1038/s41396-023-01495-w>.
- [20] D. Muñoz, I. Marcano, R. Martín-Rodríguez, I. Simonelli, A. Serrano, A. García-Prieto, M.L. Fdez-Gubieda, A. Muela, Magnetosomes could be protective shields against metal stress in magnetotactic bacteria, Sci. Rep. 10 (1) (2020) 11430, <https://doi.org/10.1038/s41598-020-68183-z>.
- [21] J.A. Diaz-Alarcón, M.P. Alfonso-Pérez, I. Vergara-Gómez, M. Díaz-Lagos, S. A. Martínez-Ovalle, Removal of iron and manganese in groundwater through magnetotactic bacteria, J. Environ. Manag. 249 (2019) 109381, <https://doi.org/10.1016/j.jenvman.2019.109381>.
- [22] S. Sannigrahi, K. Suthindhiran, Metal recovery from printed circuit boards by magnetotactic bacteria, Hydrometall. 187 (2019) 113–124, <https://doi.org/10.1016/j.hydromet.2019.05.007>.
- [23] N. Ginet, R. Pardoux, G. Adryanczyk, D. Garcia, C. Brutesco, D. Pignol, Single-Step Production of a Recyclable Nanobiocatalyst for Organophosphate Pesticides Biodegradation Using Functionalized Bacterial Magnetosomes, PLoS One 6 (6) (2011) e21442, <https://doi.org/10.1371/journal.pone.0021442>.
- [24] S.-J. Song, C.C. Mayorga-Martinez, J. Vyskocil, M. Castorala, T. Rumí, M. Pumera, Precisely Navigated Biobot Swarms of Bacteria *Magnetospirillum* magnetic for Water Decontamination, ACS Appl. Mater. Interfaces 15 (5) (2023) 7023–7029, <https://doi.org/10.1021/acsmami.2c16502>.
- [25] E.E. Khalil, T.N. Whitmore, H. Gamal-El-Din, A. El-Bassel, D. Lloyd, The effects of pesticides on anaerobic digestion processes, Environ. Technol. 12 (6) (1991) 471–475, <https://doi.org/10.1080/09593339109385032>.
- [26] C. Pozo, V. Salmerón, B. Rodelas, M.V. Martínez-Toledo, J. González-López, Effects of the fungicides maneb and mancozeb on soil enzyme activities, Toxicol. Environ. Chem. 52 (1–4) (1995) 243–248, <https://doi.org/10.1080/0272249509358265>.
- [27] X. Zhang, H. Yang, D. Wei, Z. Chen, Q. Wang, Y. Song, Y. Ma, H. Zhang, Tolerance of anaerobic digestion sludge to heavy metals: COD removal, biogas production, and microbial variation, J. Water Process Eng. 55 (2023), <https://doi.org/10.1016/j.jwpe.2023.104157>.
- [28] O. López Fernández, R. Yáñez, R. Rial Otero, J. Simó Cádára, Kinetic modelling of mancozeb hydrolysis and photolysis to ethylenebenthiourea and other by-products in water, Water Res. 102 (2016) 561–571, <https://doi.org/10.1016/j.watres.2016.07.006>.
- [29] J. Zhao, L. Gui, Q. Wang, Y. Liu, D. Wang, B.-J. Ni, X. Li, R. Xu, G. Zeng, Q. Yang, Aged refuse enhances anaerobic digestion of waste activated sludge, Water Res. 123 (2017) 724–733, <https://doi.org/10.1016/j.watres.2017.07.026>.
- [30] R. Goel, T. Mino, H. Satoh, T. Matsuo, Enzyme activities under anaerobic and aerobic conditions in activated sludge sequencing batch reactor, Water Res. 32 (7) (1998) 2081–2088, [https://doi.org/10.1016/S0043-1354\(97\)00425-9](https://doi.org/10.1016/S0043-1354(97)00425-9).
- [31] H. Xu, T. Wang, Y. Zhou, M. Zhao, W. Shi, Z. Huang, W. Ruan, Insights into the phenol disinfectant on the methane performance from wastewater by mesophilic anaerobic digestion: Single and two stages analysis, Process Saf. Environ. Prot. 170 (2023) 19–27, <https://doi.org/10.1016/j.psep.2023.11.083>.
- [32] E. Hwang, J.N. Cash, M.J. Zabik, Chlorine and Chlorine Dioxide Treatment to Reduce or Remove EBDGs and ETU Residues in a Solution, J. Agric. Food. Chem. 50 (16) (2002) 4734–4742, <https://doi.org/10.1021/fd020307c>.
- [33] Y. Xia, C. Wang, X. Zhang, J. Li, Z. Li, J. Zhu, Q. Zhou, J. Yang, Q. Chen, X. Meng, Combined effects of lead and manganese on locomotor activity and microbiota in zebrafish, Ecotox. Environ. Saf. 263 (2023) 115260, <https://doi.org/10.1016/j.ecoenv.2023.115260>.
- [34] H. Li, J. Yao, N. Min, J. Liu, Z. Chen, X. Zhu, C. Zhao, W. Pang, M. Li, Y. Cao, B. Liu, R. Duran, Relationships between microbial activity, enzyme activities and metal (loid) form in NiCu tailings area, Sci. Total Environ. 812 (2022) 152326, <https://doi.org/10.1016/j.scitotenv.2021.152326>.
- [35] J. Guan, Y. Zhang, D. Li, O. Shan, Z. Hu, T. Choi, A. Zhou, K. Qiao, Synergistic role of phenylpropanoid biosynthesis and citrate cycle pathways in heavy metal detoxification through secretion of organic acids, J. Hazard. Mater. 476 (2024) 135106, <https://doi.org/10.1016/j.jhazmat.2024.135106>.
- [36] S. Alafnan, A. Awotunde, G. Glatz, S. Adjei, I. Alrumaih, A. Gowida, Langmuir adsorption isotherm in unconventional resources: Applicability and limitations, J. Pet. Sci. Eng. 202 (2021) 109172, <https://doi.org/10.1016/j.petrol.2021.109172>.
- [37] J. Wang, K. Wang, W. Li, H. Wang, Y. Wang, Enhancing bioelectrochemical processes in anaerobic membrane bioreactors for municipal wastewater treatment: A comprehensive review, Chem. Eng. J. 484 (2024) 149420, <https://doi.org/10.1016/j.cej.2024.149420>.
- [38] G. Balcioğlu, G. Yilmaz, Z.B. Gönder, Evaluation of anaerobic membrane bioreactor (AnMBR) treating confectionery wastewater at long-term operation under different organic loading rates: Performance and membrane fouling, Chem. Eng. J. 404 (2021) 126261, <https://doi.org/10.1016/j.cej.2020.126261>.
- [39] D. Hu, H. Min, Z. Chen, Y. Zhao, Y. Cui, X. Zou, P. Wu, H. Ge, K. Luo, L. Zhang, W. Liu, H. Wang, Performance improvement and model of a bio-electrochemical system built-in up-flow anaerobic sludge blanket for treating β-lactams pharmaceutical wastewater under different hydraulic retention time, Water Res. 164 (2019) 114915, <https://doi.org/10.1016/j.watres.2019.114915>.
- [40] Y. Li, H. Yu, H. Yang, Y. Wan, Z. Pan, F. Ou, Dual-bioaugmentation strategy to simultaneously mitigate biofouling and promote methanogenesis in AnMBR, Water Res. 270 (2025) 122850, <https://doi.org/10.1016/j.watres.2024.122850>.
- [41] A.C. Haendel, J.G.M. Lubbe, Handbook of biological wastewater treatment design and optimisation of activated sludge systems, Water Intell. Online 1 (1) (2012) 11.
- [42] B. Xu, O.A.C. Cho, T.C.A. Ng, S. Huang, H.Y. Ng, Enriched auto-inducer-2 (AI-2)-based quorum quenching consortium in a ceramic anaerobic membrane bioreactor (AnMBR) for biofouling retardation, Water Res. 214 (2022) 118203, <https://doi.org/10.1016/j.watres.2022.118203>.
- [43] Y. Yang, Y. Zang, Y. Hu, X.C. Wang, H.H. Neo, Upflow anaerobic dynamic membrane bioreactor (AnDMBR) for wastewater treatment at room temperature and short HRTs: Process characteristics and practical applicability, Chem. Eng. J. 383 (2020) 123186, <https://doi.org/10.1016/j.cej.2019.123186>.
- [44] C. Wang, C. Wang, J. Liu, Z. Han, O. Xu, X. Xu, L. Zhu, Role of magnetite in methanogenic degradation of different substances, Bioresour. Technol. 314 (2020) 123720, <https://doi.org/10.1016/j.biortech.2020.123720>.
- [45] M. Zhao, J. Tang, Z. Liu, H. Miao, W. Shi, Z. Huang, W. Ruan, Coupling effect of nanoscale zero-valent iron and sodium lauroyl sarcosinate on the biogas biological upgrading from kitchen wastewater by anaerobic digestion, J. Environ. Chem. Eng. 11 (1) (2023) 109146, <https://doi.org/10.1016/j.jece.2022.109146>.
- [46] Y. Qu, Q. Guan, Y. Du, W. Shi, M. Zhao, Z. Huang, W. Ruan, Insight into the effect of rice-straw ash on enhancing the anaerobic digestion performance of high salinity organic wastewater, Chemosphere 340 (2023), <https://doi.org/10.1016/j.chemosphere.2023.139920>.
- [47] Q. Gao, O. Zhao, K. Wang, X. Li, H. Zhou, J. Ding, L. Li, Promoting methane production during anaerobic digestion with biochar: Is it influenced by quorum sensing? Chem. Eng. J. 483 (2024) 149268, <https://doi.org/10.1016/j.cej.2024.149268>.
- [48] Y. Zhong, J. He, F. Wu, P. Zhang, X. Zou, X. Pan, J. Zhang, Metagenomic analysis reveals the size effect of magnetite on anaerobic digestion of waste activated sludge after thermal hydrolysis pretreatment, Sci. Total Environ. 851 (2022) 158133, <https://doi.org/10.1016/j.scitotenv.2022.158133>.
- [49] C. Wang, Y. Liu, S. Jin, H. Chen, X. Xu, Z. Wang, B. Xing, L. Zhu, Responsiveness extracellular electron transfer (EET) enhancement of anaerobic digestion system during start-up and starvation recovery stages via magnetite addition, Bioresour. Technol. 272 (2019) 162–170, <https://doi.org/10.1016/j.biortech.2018.10.013>.
- [50] Z. Chi, L. Zhang, S. Ju, W. Li, H. Li, X. Ren, Vanadium bioreduction in an ethane-based membrane biofilm reactor: Performance and mechanism, Chem. Eng. J. 499 (2024) 156468, <https://doi.org/10.1016/j.cej.2024.156468>.
- [51] M. Wang, J. Li, S. Ning, X. Fu, X. Wang, L. Tan, Simultaneously enhanced treatment efficiency of simulated hypersaline azo dye wastewater and membrane antifouling by a novel static magnetic field membrane bioreactor (SMFMBR), Sci. Total Environ. 821 (2022) 153452, <https://doi.org/10.1016/j.scitotenv.2022.153452>.